FACULTY OF ENGINEERING AND ARCHITECTURE

Development of antibacterial TiO_2 coatings on titanium implants by plasma electrolytic oxidation

Renee Coryn
Student number: 01408564

Supervisors: Prof. dr. ir. Nathalie De Geyter, Prof. dr. ir. Kim Verbeken
Counsellor: Monica Thukkaram

Master's dissertation submitted in order to obtain the academic degree of
Master of Science in Biomedical Engineering

Academic year 2018-2019

GHENT UNIVERSITY

FACULTY OF ENGINEERING AND ARCHITECTURE

Development of antibacterial TiO_2 coatings on titanium implants by plasma electrolytic oxidation

Renee Coryn
Student number: 01408564

Supervisors: Prof. dr. ir. Nathalie De Geyter, Prof. dr. ir. Kim Verbeken
Counsellor: Monica Thukkaram

Master's dissertation submitted in order to obtain the academic degree of
Master of Science in Biomedical Engineering

Academic year 2018-2019

GHENT UNIVERSITY

Preface

Writing the master dissertation "Development of antibacterial TiO_2 coatings on titanium implants by plasma electrolytic oxidation" has been a journey from beginning to end. This thesis about the development of an antibacterial TiO_2 coating and the analysis of its chemical, biological and mechanical properties was conducted to order to obtain the degree of master's in science in biomedical engineering.

The research question was imposed by my two promotors Kim Verbeken and Nathalie De Geyter whom I would like to thank for challenging me with this interesting topic. Special gratitude should be given to the professional guidance of my supervisor Monica Thukkaram not only for her device training throughout this year but also for her expertise, advice and especially her valuable feedback.

Furthermore I would also like to mention the faculty members who contributed somehow in the accomplishment of this master dissertation. Elien Wallaert and Tim De Seranno for their supervision in the material science department in Zwijnaarde, Pieter Cools and Sheida Aliakbarshirazi for the aid with the repair and use of devices in the department in absence of my supervisor and last but not least Tim Poelman for his technical support.

At last I would like to thank my friend Nathalie, my sister Astrid and my mother Karien for their encouragement, the from time to time needed diversion and their enduring support during this research journey. The latter deserves special recognition for her everlasting mental and financial support in the achievement of this master degree.

I hope you enjoy your reading.

Best regards
Renee Coryn

Abstract

Development of antibacterial TiO_2 coatings on titanium implants by plasma electrolytic oxidation

R. Coryn, Ir. M. Thukkaram, Prof. Dr. ir. K. Verbeken, Prof. Dr. ir. N. De Geyter

Implant associated infections remain one of the main issues limiting the performance of titanium implants. The difficulty in handling these postoperative infections urges the need for new preventative measures. In this master dissertation silver and copper doped porous TiO_2 coatings enriched in calcium and phosphorous were deposited on titanium disc by plasma electrolytic oxidation. Surface properties of the deposited coating were studied by XPS, SEM-EDX and AFM. In vitro antibacterial assay was performed to evaluate the antibacterial properties of the coating. In addition a cytotoxicity study was performed using MTT and live/dead staining. After PEO, a porous coating morphology was obtained resembling a hydroxyapatite like coating. From SEM-EDX and XPS it was observed that both calcium and phosphorous were present at the top surface and also closer to the bulk. Furthermore, a Ag/Cu distribution was observed both on the surface and inside the porous TiO_2 coating. The release rate of these antibacterial elements was investigated for about two weeks using ICP-MS. The treated titanium disc exhibited excellent antibacterial activity against both E. coli and S. aureus. In addition sufficient cell viability was observed which indicates the biocompatibility of the TiO_2 coating with an upper limit regarding the silver concentration. At last mechanical tribology testing concluded the increased friction coefficient and reduced scratch depth for the treated titanium compared to the untreated. Favourable surface, biological and mechanical experiments promote further research regarding the effective use of the designed antibacterial TiO_2 coated titanium implants for orthopaedic applications.

Keywords

Titanium, Antibacterial, Biocompatible, Plasma Electrolytic oxidation, Silver acetate, Copper acetate

Development of antibacterial TiO_2 coatings on titanium implants by plasma electrolytic oxidation

R. Coryn, Ir. M. Thukkaram, Prof. Dr. ir. K. Verbeken, Prof. Dr. ir. N. De Geyter

Infection is one of the major problems in orthopaedics leading to implant failure. Up until today the most common treatment remains administration of antibiotic drugs and implant removal. Though several strategies were incorporated to prevent infection, still there is a pressing need to develop antibacterial coatings that support tissue integration and growth.

I. INTRODUCTION

Titanium and its alloys are mostly used as implant materials due to their superior natural biocompatible properties over other metals. Their mechanical properties favour their use in load bearing orthodontic and orthopaedic applications. Despite their great success, implant related infections remain a major issue. These originate from planktonic bacteria that colonize at the implant's surface where a biofilm is formed due to the transformation of these free-floating bacteria to sessile bacteria. The latter become embedded in a slimy extracellular matrix after adhesion to the implant surface. Due to this transformation the bacteria can withstand host immune responses and become resistance to antibiotics, therefore the only possible solution remains implant removal and re-implantation [1]. This not only has an adverse impact on the quality of life of the patient but also increases healthcare costs. Incorporation of antibiotic particles in the implant surface may solve this problem. Several strategies have been studied, such as antibacterial cements, antibiotics loaded in ceramic or polymer coatings and organic antimicrobial particles directly absorbed to the implant surface or incorporated in a coating. The most efficient technique remains inclusion of inorganic antimicrobial particles like copper, gold, silver and zinc through several procedures [2]. A promising technique is plasma electrolytic oxidation, an anodic oxidation process where the sample is immersed in an electrolytic bath containing dissolved salts. This simple method results in the formation of a thick, hard dioxide layer on the titanium surface. Due to the combined current and high voltage, plasma is created at the surface causing oxidization and formation of a nano-structured porous layer [3]. Calcium, phosphorous and antibacterial particles can be added to the electrolyte respectively to promote osteogenic properties and to restrict implant infections. Doping these elements in the TiO_2 layer alters the surface properties of the implant [4].

II. EXPERIMENTAL TECHNIQUES

A. PEO

Pure grinded and polished titanium disks from L&D Techniek NV, 12 mm in diameter and 3 mm in thickness were subjected to a PEO process at 450 V for 5 minutes in an electrolyte containing 5 g/L calcium ($Ca_5(PO_4)_3OH$) and 2 g/L phosphorous (NaH_2PO_4-$2H_2O$) along with silver ($AgOOCCH_3$) or copper ($Cu(OOCCH_3)_2$) acetate with a concentration varying between 0,1 g/L and 1 g/L. Afterwards all samples were washed with distilled water and air dried.

B. Chemical & morphological characterization

Surface morphology and composition were examined by SEM-EDX (JSM-6010 PLUS/LV, JEOL & JSM-7600F FEG, JEOL) at an accelerating voltage of 7 kV and a working distance of 11 mm. Element analysis was performed through XPS on a PHI 5000 Versaprobe II spectrometer and quantified by MultiPak software. An XE-70 AFM system with a silicon based cantilever was used in non-contact mode to study the surface topography and to determine surface roughness.

C. Biological characterization

First of all the silver ion release kinetics were monitored by NexION 350 ICP-MS measuring the concentration of released silver. The silver doped disks were immersed in 20 ml of distilled water at 37 °C for varying time periods. The antibacterial properties of the coatings were evaluated against Escherichia coli ATCC 25922 and Staphylococcus aureus ATCC 6538 after an incubation period of 24 hours at an elevated temperature of 37 °C. The plate count method was used to determine the number of colony forming units. Furthermore cell viability was tested against osteogenic MC3T3 cells seeded on through UV light sterilized treated and untreated disks at a density of 50 000 cells cultivated at a temperature of 37 °C. Cell adhesion, proliferation and viability were measured after 1 and 7 days and TCPS plates were used as a positive control. The samples were incubated for 4 hours in MTT solution to assess the mitochondrial activity. Live-dead immune fluorescence microscopy (Olympus; IX 81) and SEM after cell fixation were used to analyze cell morphology and viability upon adhesion.

D. Mechanical characterization

Finally, mechanical properties were characterized by the coefficient of friction obtained from the pin-on-disk small scale tribometer (PoD ASTM G132). A steel indenter with a diameter of 8 mm was operated at a sliding speed of 3 mm/s carrying a load between 1 N and 10 N.

III. RESULTS

A. XPS

XPS analysis confirmed the presence of the antibacterial silver or copper in the TiO_2 coating. From Figure 1 it can be seen that the Ag and Cu at% increases with increasing electrolyte concentrations. Furthermore both calcium and phosphorous incorporation was proven with a Ca/P ratio between 1 and 1,5 for the silver doped layer and a ratio around 0,5 for the copper doped, all below the desired 1,67 hydroxyapatite ratio.

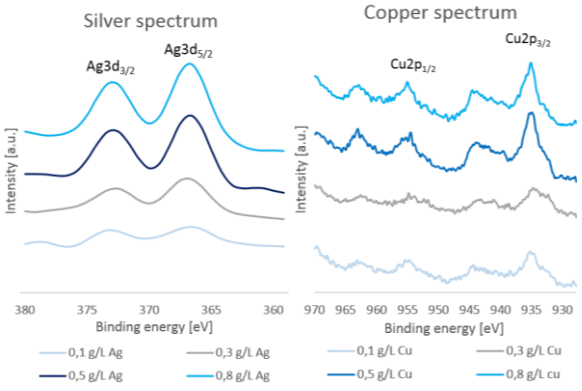

Figure 1 - Detailed spectra of the peak increase at the binding energy of the antibacterial particles. Left: Silver doped TiO_2. Right: Copper doped TiO_2.

B. SEM-EDX

EDX element analysis confirmed the presence of calcium, phosphorous and copper or silver in the TiO_2 layer. The detected Ca/P ratio however appeared lower compared to the XPS data. The principle underlying both

techniques results in a different analysis depth. While XPS only determines the chemical composition of the upper 5 nm, EDX allows element analysis over the entire depth of the TiO_2 layer. Therefore, it can be presumed that calcium is situated rather at the surface of the layer easing its detection through XPS. Cross-sectional EDX analysis exposed the phosphorous enrichment near the bulk and calcium presence at the surface, both in oxygen rich areas. SEM analysis given in Figure 2 was used to examine the surface morphology of the coating and to compare it with hydroxyapatite coatings obtained from other techniques. Not only a great resemblance was found with the through PEO obtained TiO_2 layer, independent of the electrolyte composition, but also both micro and nanoscale porosity were detected, possibly favouring the release kinetics. Preservation of this coating morphology under aqueous in vivo conditions was proven from SEM images.

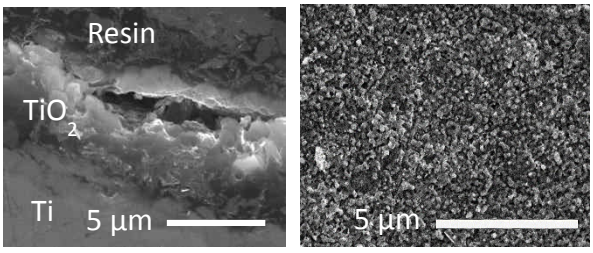

Figure 2 - SEM analysis of the surface morphology of the porous TiO2 layer. Left: Cross-sectional analysis. Right: Surface analysis.

Analysis of backscattered electrons given in Figure 3 illustrated the advantage of the incorporation of metallic salts over nanoparticles as a non-agglomerated rather homogeneous distribution of the silver and copper elements was found. Further surface topology analysis performed with AFM resulted in a surface roughness around 100 nm independent of the concentration or nature of the antibacterial element.

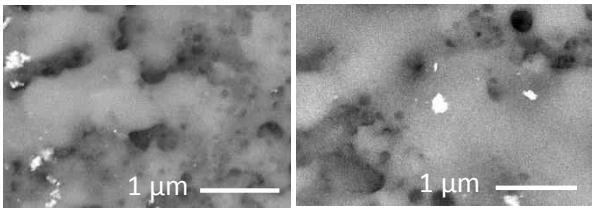

Figure 3 - Backscattered electron SEM images enlighten the heavier particles in the porous TiO_2 coating. Left: Silver doped TiO_2. Right: Copper doped TiO_2.

C. ICP-MS

ICP-MS was used to quantify the release kinetics of the antibacterial particles during 17 days as illustrated in Figure 4. Increasing silver electrolyte concentrations results in a greater amount of released silver ions. Within the first hours a quick burst release of silver ions is detected while saturation is expected after several days. A prolonged ICP-MS analysis is needed to determine the complete time range of silver release and compare this to the antibacterial needs of the implant.

D. Antibacterial analysis

The efficiency of the release was examined though antibacterial testing on E. coli and S. aureus bacteria of which the results are given in Figure 5. The presence of silver and copper particles induced a substantial decrease in bacterial counts with an increasing bacterial reduction at higher silver or copper concentrations while no bacterial reduction was seen on the untreated titanium plates. An inhibition of over 99% was obtained even for the smallest concentration, which is sufficient to speak of complete antibacterial activity. Overall, a slight superiority of silver over copper can be seen regarding its antibacterial activity, this difference however remains restricted to a minimum.

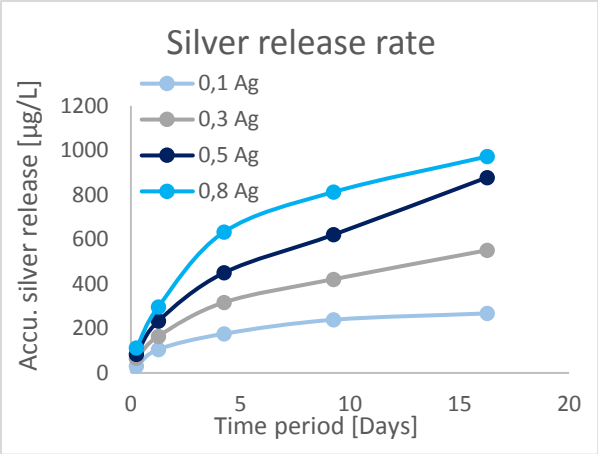

Figure 4 - ICP-MS analysis illustrating the silver release kinetics in distilled water at 37 °C during 17 days.

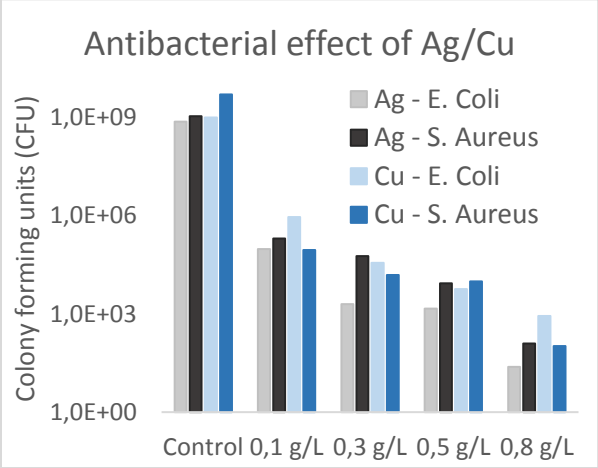

Figure 5 - Reduction in the number of E. coli and S. aureus bacteria by the silver or copper acetate incorporated in the titanium dioxide layer.

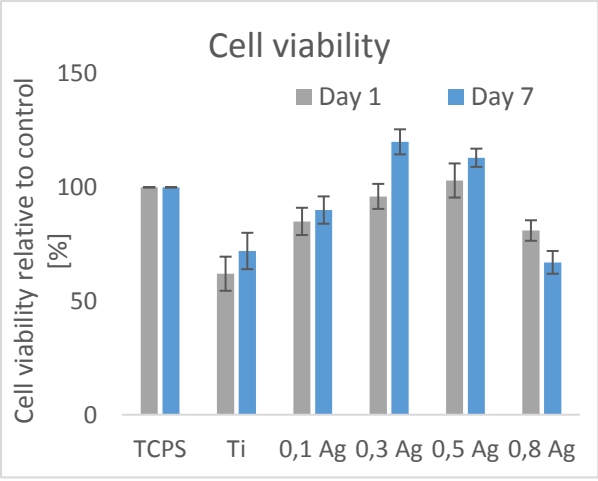

Figure 6 - MTT analysis indicating cell viability relative to TCPS of the untreated Ti and the TiO2 layer under varying antibacterial silver conditions.

E. Cytotoxicity analysis

The biocompatible properties of any surface are influenced by its surface properties and its chemical constituents. A decrease in WCA from 70° to 15°-20° after coating indicated an increase in hydrophobicity enabling cell spreadability. Figure 7 illustrates the difference in cell morphology upon adherence on an untreated versus a treated titanium plate. In case of control titanium, cells exhibit a round morphology indicating a low cell-surface affinity while an elongated spindle cell morphology indicates the favoured cell-surface interaction for the treated samples. Great initial adherence and increased cell proliferation over time were observed for the PEO treated titanium surfaces.

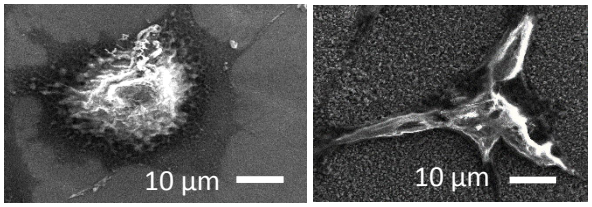

Figure 7 - SEM images taken 7 days after seeding illustrating cell-surface interactions. Left: Untreated titanium plate. Right: Silver doped TiO_2 layer.

Cytocompatibility was further analysed through MTT to quantify the number of viable cells. From Figure 6 it can be stated that all layered samples are considered to be biocompatible according to the ISO standard [5]. The biocompatibility is not only obtained from the incorporated calcium and phosphorous but also from the antibacterial particles. While a restricted amount of antibacterial particles appears to up-regulate certain cell proteins, a too large occupancy of these particles downregulates the cell viability which is seen from the induced toxicity of the 0,8 g/L Ag sample. A too large

concentration results in an uncontrolled reaction between these antibacterial particles and certain macromolecules triggering apoptosis. Fluorescent live-dead staining confirmed the increased cell viability on the treated titanium samples in case of low silver concentrations and a decreased viable cell density was observed for samples containing high silver concentrations.

F. Scratch test

A mechanical pin-on-disk tribology test indicated the advantageous properties of the TiO_2 layer regarding wear resistance compared to untreated titanium. The rather rough porous surface structure led to an increases coefficient of friction compared to bulk titanium. The restricted indent depth measured through AFM forecasts successful use of the coating in bone screw applications.

IV. CONCLUSION

The objective of the research was to develop both an antibacterial and biocompatible porous titanium dioxide layer through plasma electrolytic oxidation. Calcium and phosphorous were detected by XPS and EDX to a sufficient extent to promote osteogenic properties. Cross sectional analysis revealed the inhomogeneous particle distribution over the depth of the coating. The surface is enriched in calcium while phosphorous is located close to the bulk. Silver and copper appear uniformly distributed over width and depth of the coating.

SEM and AFM exposed the porous coating morphology favouring the release rate of Ag/Cu. Quantification of the kinetics through ICP-MS indicates a quick burst release with an expected saturation after several days imposing a required minimal concentration. Complete antibacterial activity against E. coli and S. aureus was measured during the burst release in the first 24h.

Reduced cell viability resulting from a too high silver concentration induces an upper limit to the concentration increase needed to preserve the particle release. MTT and immune fluorescence illustrated the toxic side effects of the coating obtained from a 0,8 g/L Ag electrolyte concentration. Small concentrations on the other hand up-regulate cell viability and favour cell-surface interactions characterised by a spindle cell morphology.

The surface roughness associated with the coating increases its wear resistance lowering the risk for abris release. This favours the use of the coating in orthopaedic applications.

V. FUTURE WORK

Prolonged ICP-MS analysis is needed to determine the point of saturation. Extra mechanical testing should be performed, especially under in vivo conditions. Furthermore, PEO process parameters should be adapted and optimised to allow layer deposition on 3D shaped samples instead of flat plates.

REFERENCES

[1] L. Visai *et al.*, “Titanium oxide antibacterial surfaces in biomedical devices,” *Int. J. Artif. Organs*, vol. 34, no. 9, pp. 929–946, 2011.

[2] L. Zhao, P. K. Chu, Y. Zhang, and Z. Wu, “Antibacterial coatings on titanium implants,” *J. Biomed. Mater. Res. - Part B Appl. Biomater.*, vol. 91, no. 1, pp. 470–480, 2009.

[3] Y. Wang, H. Yu, C. Chen, and Z. Zhao, “Review of the biocompatibility of micro-arc oxidation coated titanium alloys,” *Mater. Des.*, vol. 85, pp. 640–652, 2015.

[4] H. Cao and X. Liu, “Activating titanium oxide coatings for orthopedic implants,” *Surf. Coatings Technol.*, vol. 233, pp. 57–64, 2013.

[5] “International Organization for Standardization,” 2017. [Online]. Available: https://www.iso.org/standard/36406.html. [Accessed: 17-May-2019].

Content

List of figures

List of tables

List of abbreviations

AFM	Atomic force microscopy
BCC	Body centred cubic
CFU	Colony forming units
EDX	Energy dispersive X-ray spectroscopy
FCC	Face centred cubic
HCP	Hexagonally closed packed
ICP-MS	Inductively coupled plasma mass spectroscopy
MAO	Micro-arc oxidation
MTT	3-(4,5-dimethylthiazol-2-yl)-2,5-diphenyltetrazolium bromide.
PBS	Phosphate-buffered saline
PEO	Plasma electrolytic oxidation
ROS	Reactive oxygen species
SEM	Scanning electron microscopy
TCPS	Tissue culture polystyrene
XPS	X-ray photoelectron spectroscopy

Literature study

1 Introduction

Over the past years a lot of resources have been invested in the healthcare system, including medical implants. Medical implants include all devices, materials and tissues placed inside or on the surface of the body. Their main purpose is to monitor body functions, deliver drugs or support organs, tissue and bones. Prosthetics on the other hand are medical implants intending to replace one or several missing body parts for a restricted or an infinite period of time [6]. The material from which medical implants are composed depends on their application. Polymers, metals, ceramics, biological tissues and composite materials are commonly used materials for medical implants [7]. Certain risks are related to medical implants, occurring over their complete lifetime starting from the surgical risks on the operating table to post-surgical problems eventually leading to implant failure. All surgical procedures are related to risks of which infection is the most common one indicated by pain, redness and swelling at the surgical site [6]. Most obvious treatment for these surgical induced infections up until today is the administration of antibiotic drugs.

2 Metallic implants

Metallic implants are the primary biomaterials used for joint replacements and they are becoming increasingly important. Commonly used metallic implants for orthopaedic applications are stainless steel, titanium, titanium alloys and cobalt chromium alloys. These metallic materials have several properties such as high strength, high fracture toughness, hardness, corrosion resistance and biocompatibility which make them an excellent choice for the orthopaedic implants. An increase in aging population, vulnerable to osteoarthritis and rheumatoid arthritis and with a desire to maintain their quality of life and level of activity, has led to a rising need for medical implants. Additionally these elderly require special consideration in implant treatment due to their systemic health problems. A variety of

synthetic, natural, metallic, ceramic, polymer and hybrid materials allow material selection for specific treatments. The new arising technique of 3D printing contributes even more to this personalised medicine. For load bearing orthopaedic applications both permanent and biodegradable metals remain the material of choice [8]. Depending on the application in which the metal is used, certain requirements should be fulfilled. The basic requirement imposes biocompatibility and non-toxicity, of both the bulk metal and the coating applied to it. Furthermore, a great resemblance between the physical and mechanical properties of the human tissues and bones and the metal implant is imposed. Due to the high load bearing capacity of orthopaedic implants it is essential it possesses better mechanical stability than other implant surfaces. These mechanical properties should furthermore be adapted to the function of the body part. For example bone implants in the lower limbs should be stronger due to the higher loads these limbs carry compared to other bones [1].

Permanent implants require both long-term stability under in vivo conditions and preservation of mechanical properties. A too stiff implant should be avoided to prevent stress shielding. This will generate weary bones since the bone doesn't feel the actual load anymore due to the presence of these stiff metal implants. Due to this, healing will never generate bones as strong as they originally were while bone regeneration in their natural behaviour is targeted [1]. Preservation of these properties is however restricted by wear, friction and the aggressive microenvironment resulting in the problematic release of metallic ions causing tissue damage and inflammatory reactions. Well known bio-inert metals are stainless steel, cobalt chromium and titanium alloys. Stainless steel is mostly used for its increased corrosion resistance under reactive in vivo conditions reducing post-surgical complications [8]. Secondly the formability of steel is favoured over other metals, allowing both bulky structures and complex 3D printed implants [1]. It's widely used for screws, fracture plates and other temporary support structures [8]. The stiffness properties (205 GPa) and resulting stress shielding however restrict its use in permanent orthopaedic applications [1]. Titanium alloys are considered superior to stainless steel due to their higher strength to weight ratio hence favouring their use in high load bearing applications. Furthermore titanium surface promotes cell integration due to its naturally formed dioxide layer [8]. Titanium is the biocompatible metal with the stiffness (127 GPa) most resembling that of bone (17 GPa). Moreover can the stiffness of pure

titanium be reduced to 60 GPa by the addition of certain alloys. This rather limited deviation in stiffness properties is advantageous regarding the induced stress concentrations at the bone-implant interface. Magnesium and its alloys are also widely used in orthopaedic applications due to the greater resemblance of their elasticity modulus (45 GPa) to bones. This metal however has the disadvantage of being very reactive and corrosive. Another characteristic of orthopaedic applications is their cyclic loading, inducing the need for implant materials with high fatigue strength [1]. Cobalt based metals are preferred for their great fatigue properties and their high wear resistance both favouring its use in artificial hip joints. Furthermore it possesses high strength combined with great ductility. The downside to this is the increased stress shielding compared to other metal alloys. Cobalt chromium is mostly used for structures without direct contact to the bone due to their inferior biocompatibility [8].

When complete tissue regeneration is desired biodegradable metals are preferred for fracture fixation. Magnesium, iron and zinc can control degradation with adequate mechanical strength. Not only are the mechanical properties of resorbable metals superior over those of polymers but also the degradation products can be metabolised by the host cells hence decreasing the inflammatory response [8].

3D printing not only allows the construction of specific implants mimicking the patient's anatomy but also provides a way to manipulate mechanical properties to optimally mimic the human body. The porosity created by 3D printing reduces structural stiffness diminishing stress shielding. Secondly it also promotes osseointegration and vascularization by manipulation of the size, shape and orientation of the pores. All of these result in reduced procedure time and improved surgical outcome. A price however has to be paid for these highly desirable properties as the computer aided design, the needed CT scans, the modelling and the printed prototypes add up to the final price tag of the implant [8].

3 Problems associated with metallic implants

3.1 Biocompatibility

The biocompatibility of a medical device is directly related to its chemical composition and surface properties. The fundaments for both these properties lie in the device design process. Most importantly the design aims to mimic the structure and properties of its replacement tissue. Later design modification is induced after analysis of its performance, efficacy and safety of the medical implant. The latter is tested via several biological tests evaluating both biocompatibility and cytotoxicity. Generic biological test methods differ between medical implants since biological reactions that define the success of one device may not be in line with another device with a different application [7].

3.2 Device related infections

An increasing number of clinical procedures requires the use of medical implants. Although medical implants have their own advantages, material induced infection and foreign body response remain major challenges for implanted medical devices [2]. Annually about two million cases of nosocomial infections occur, of which half are related to indwelling devices. These nosocomial infections include all infections acquired in a hospital or in another health care facility [2]. Figure 1 represents the schematic illustration of a healthy verses an infected screw indicating the redness and inflammation on the infected area.

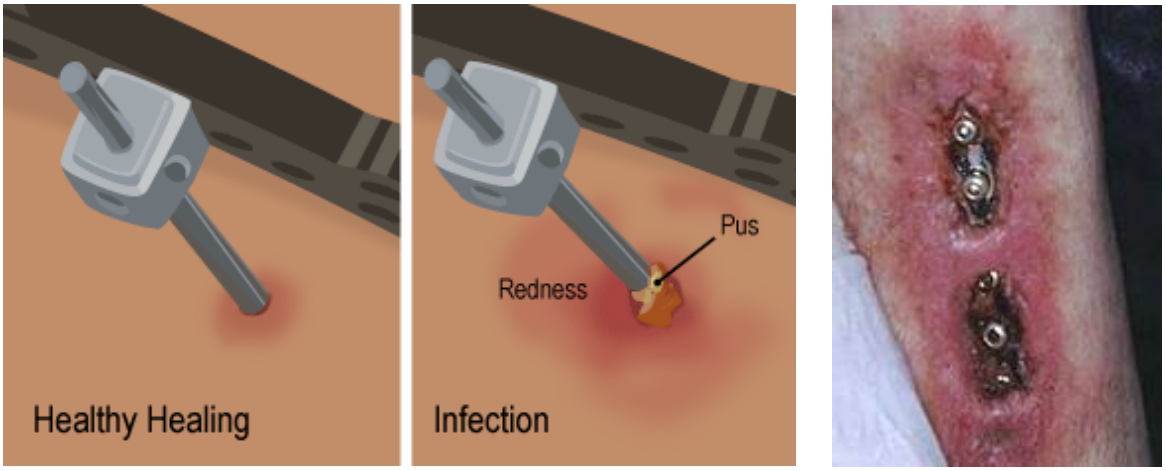

Figure 1 *- Infected implant. Left: Schematic illustration of infected bone screw* [9]*. Right: Image of infected bone screws in the lower limb clearly indicating the infection induced redness* [10]*.*

Infections originate from the free-floating planktonic bacteria that colonize at the implant's surface where they form a matured biofilm as illustrated in Figure 2. These bacteria originally float in liquid medium but after adhesion to the surface they transform to sessile bacteria. The latter are the bacteria living in biofilms where they become embedded in a slimy extracellular matrix composed of extracellular polymeric substances [2]. Bacteria in a biofilm are surrounded by a gelly exopolysaccharide matrix [11]. Due to this transformation the bacteria can withstand host immune responses and become resistant to antibiotics. First of all, the formation of exopolymeric substance prevents the entry of antibacterial agents into the bacteria due to its retarded diffusion [2]. Secondly bacteria in the biofilm behave differently due to their limited nutrition. Hence the antibiotic therapy is insufficient to prevent biofilm infections and may only prevent planktonic cells released from the biofilm [11].

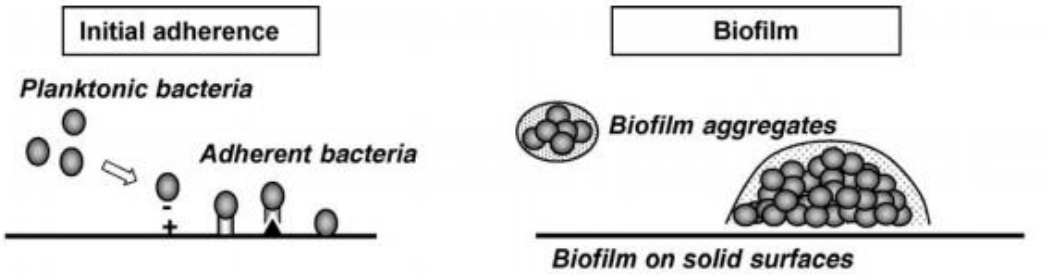

Figure 2 *– Schematic representation of bacterial adherence on the surface of the implant material resulting in biofilm formation* [12]*.*

Gram-positive bacteria such as Staphylococcus aureus and Staphylococcus epidermidis [11,13], and gram-negative bacteria such as Escherichia coli [13] and Pseudomonas aeruginosa [11] belong to the most important pathogens related to material induced infections. All these bacteria are characterised by a cell wall enclosing their outer cell membrane. Polysaccharides and peptides, shortly peptidoglycan, make up this wall needed for bacterial survival. A distinction can be made between two types: gram-positive and gram-negative facades depending on their reaction to gram staining. Gram-positive bacteria are characterised by many peptidoglycan layers resulting in a thick wall. Gram-negative bacteria on the other hand are made of only a few layers [14].

Staphylococcus aureus is normally present in the skin and affecting all mammalian species. It is one of the most common causes of post-surgical or post-injury infections [15]. Escherichia coli is normally present in the intestines of both human and animals causing intestinal infections resulting in abdominal pain, diarrhea and fever. Most frequent E. coli infections result from ingestion of contaminated food or water [16]. Pseudomonas aeruginosa is well known for its antibiotic resistance caused by the diminished permeability of the outer bacterium cell membrane [17].

4 Titanium based implants

The natural biocompatible properties of bulk titanium are superior over other metals mainly due to the naturally formed titanium dioxide surface layer. Moreover its corrosion resistance is superior over stainless steel and cobalt-chromium alloys. Titanium implants are often used in orthopaedic applications since the low stiffness (127 GPa) of this metal resembles actual bone properties reducing the risk for stress shielding. Static contact applications are preferred over dynamic loadings due to the limited wear resistance of titanium. The naturally formed biocompatible hard oxide layer tends to form debris when moving against other metallic material. As a result titanium dioxides will be released in the body to other sites than the original implant [1]. This may eventually result in the entrance of these particles in the blood stream after which they can accumulate in vital organs. In the worst case these titanium debris accumulate in the brain causing brain damage and neurotoxicity [18].

Titanium is characterised by its allotropic transformation at 885 °C from hexagonal closed packed (HCP, α-titanium) to body centred cubic (BCC, β-titanium). This transformation improves the ductility of pure titanium. In the BCC structure the twelve favoured slip systems are not closely packed therefore the ductility of this structure is inferior to the face centred cubic structure in which the twelve favoured slip systems are closely packed easing the movement of dislocations. This high temperature BCC structure is however favourable over the natural HCP structure of titanium since the number of favourable slip systems in the latter is limited to only three. Above all, these HCP slip systems are not closely packed and they all lie in the same plane not allowing dislocation movement in all directions [19].

Properties of titanium may be further improved by using this structure transition and decreasing its brittle behaviour. This is done by the addition of alpha and beta alloys stabilizing the BCC structure at room temperature, better known as solid solution strengthening. The beta alloys are obtained by the addition of substitutional elements that dissolve in the beta phase such as molybdenum (Mo), vanadium (V) and niobium (Nb). These alloys have an advantage over pure titanium regarding cold formability and hardenability. Whereas alpha phase stabilizing substitutional elements are aluminium (Al), copper (Cu), nickel (Ni) and tin (Sn). Pure alpha alloys are however not used in medical applications due to their low formability resulting from the HCP-structure. Mostly titanium alloys contain both alpha and beta stabilizers since it reduces titanium's brittleness and allows precipitation hardening [1].

Ti6Al4V alloy is mostly used in orthopaedic applications for its excellent biocompatibility, toughness, low density and corrosion resistance. However, it also has its disadvantages. It has been reported that vanadium and aluminium elute from titanium years after implantation inducing carcinogenic effects and stimulation of Alzheimer's disease [20]. As a response to these effects new αβ-titanium alloys are rising in medical applications. Interesting replacements are TiNb13Zr13 and near-β TiNb30 which provide low elastic modulus and corrosion resistance favouring their use for long-term implants [21].

4.1 Applications

Titanium implants are used in several practices ranging from dental applications to pacemakers and orthopaedic implants, a few examples are given below in Figure 3. In dentistry commercially pure titanium is mostly preferred over its alloys for crowns, bridges and dental prosthesis despite Ti6Al4V being stronger. The main disadvantage of the latter is its low wear resistance and lower corrosion resistance, making it rather unfavourable for dental applications. Three main dental implant types may be distinguished: osseo-integrated implants, zygomatics and mini-implants for orthodontic purposes. The first category includes all applications with a direct bone-implant contact under loaded conditions. In orthodontic applications the titanium implants serve as a temporary anchorage. Finally also atrophic maxilla may be treated with dental implants, namely zygomatic fixtures [22]. Subsequently titanium is also used for the encapsulation of the pulse generator in pacemakers. The advantage of titanium lies in its ability to shield electromagnetic interference therefore the patient is still allowed to use other electrical devices such as a cell phone or a microwave [1]. Finally titanium and its alloys are often used in orthopaedic applications as the replacement of hard tissue like artificial hip joints, artificial knee joints, bone plates and screws for fracture fixation [22]. For these applications bone ingrowth is favoured to stabilize the implant, hence this is obtained via surface modification techniques such as hydroxyapatite like coatings on titanium substrates [23].

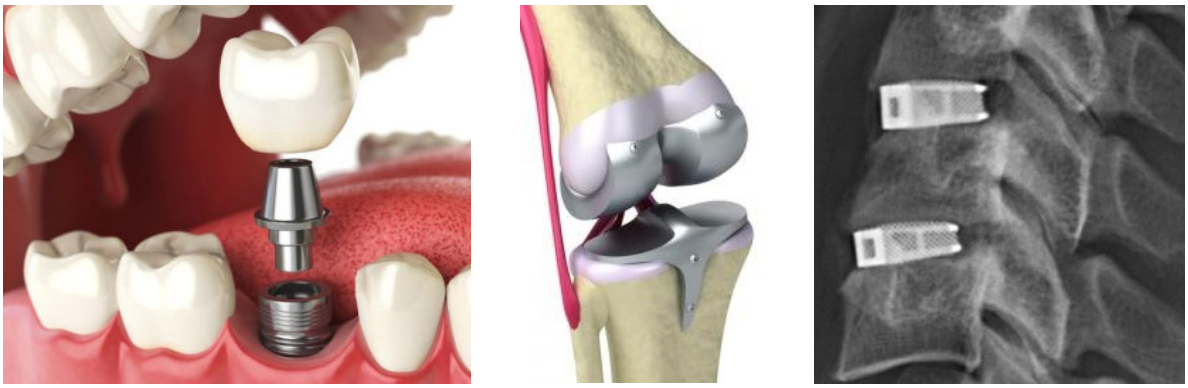

Figure 3 *- Applications of medical titanium implants. Left: Root of dental replacement* [24]*. Middle: Artificial knee joint* [25]*. Right: 3D printed intervertebral disc* [26]*.*

5 Antibacterial coatings on titanium implants

Both mechanical and biocompatible properties of titanium contribute to its use in medical applications. As already stated, one of the main complications associated with titanium-based implants are implant associated infections. Since these infections are difficult to treat, prophylactic measures are needed to prevent implant removal. Incorporating an antibacterial element into the titanium can impede the formation of a biofilm at the implant surface. Antibacterial coatings on titanium implants can be performed via several methods as indicated in Figure 4 [3].

Two important factors should be noted for the fabrication of an antibacterial coating. Firstly, the coating should not restrict tissue integration and preferably it should even promote it. Secondly the coating should be adapted to its environment and its associated bacteria, the antibacterial coating should be tailored depending on the bacterial ecosystem [3].

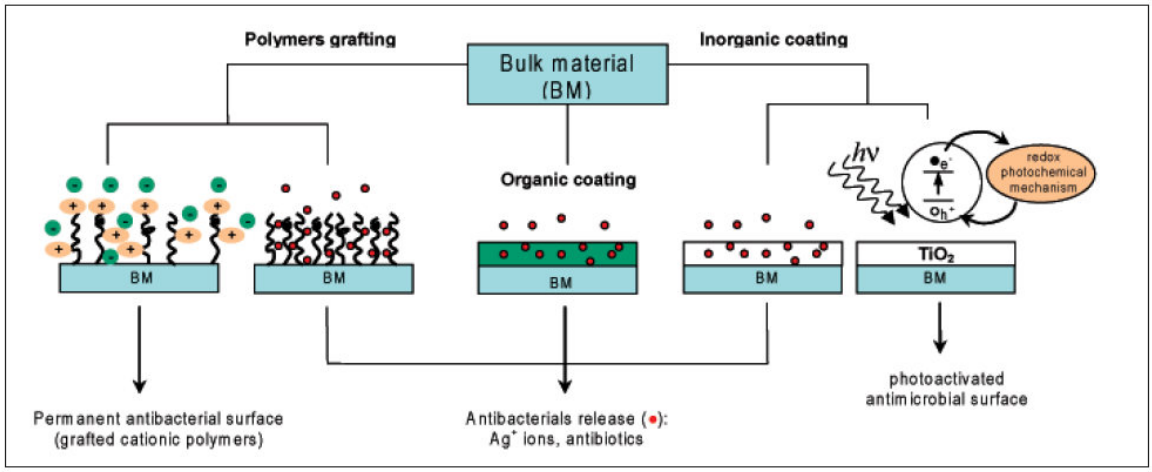

Figure 4 *- Surface modifications of medical implants to induce and increase antibacterial properties* [2].

5.1 Antibiotic coatings

Antibiotic prophylaxis is most commonly used to prevent postsurgical infections. However oral intake of antibiotics has the disadvantage that only a limited amount is delivered at the target site. In order to overcome this problem on-site delivery mechanisms were performed. Since the early 1970's local prophylactic antibiotics have been delivered on site after total joint

arthroplasty via incorporation of antibacterial segments in bone cement [27]. Despite the great effect of this incorporation, antibacterial cements are barely used anymore. This is due to the better and faster results obtained by cementless bone implants compared to cement counterparts. From this shift in implant technique the need arose for the development of antibiotic coatings on the titanium implant itself [28].

A first attempt to integrate antibiotics was done with gentamicin. This antibiotic was chosen for its broad antibacterial spectrum. Gentamicin was initially merged in hydroxyapatite coatings which are known for their high biocompatibility and their promotion of osseo-integration [3]. The downside of this antibiotic hydroxyapatite coating is that despite its high thermostability gentamicin can't be added during the coating process due to the high temperature needed for plasma spraying. Hence incorporation results from physical absorption after a dipping procedure. This technique is however not optimal as the antibiotic distribution is rather limited resulting in a burst release of about 80-90% of the antibiotics in the first hour. Therefore an efficient coating technique is required to improve its prophylaxis antibiotic properties [19,20].

Due to the disadvantages illustrated above a new technique was developed to produce hydroxyapatite and other calcium phosphate coatings. Antibiotics are added to a supersaturated solution of calcium phosphates in which the titanium is immersed at ambient temperatures [31]. Addition of the antibiotics to the solution results in coprecipitation with the calcium phosphate crystals gradually forming a layer on the titanium surface. This new techniques allows a greater antibiotic content in the biocompatible coating, the release rate however appeared barely retarded compared to the previous technique [3].

Apart from the ceramic calcium phosphate coatings also polymer coatings can be utilized for controlled release of antibiotics. It has been proved that gentamicin antibiotics can be loaded in biodegradable poly (D,L-lactide) polymers and that they're efficiently released. The release rate is slower than from calcium phosphates coatings with about 80% of the antibiotics released during the first two days. This elution is however still too fast for the orthopaedic applications in which titanium implants are mostly used [32].

Besides the use of polymers as drug releasing compounds, they are also of interest due to their ability to covalently bind certain drugs to the implant surface. Vancomycin antibiotics have proven the efficiency of this technique as they can covalently bound to titanium surfaces and their antibacterial activity is preserved over eleven months. Besides their long-lasting antibacterial activity another advantage is the diminished amount of side effects due to the fact that the antibacterial drugs can't be delivered to non-critical areas in the human body. A disadvantage on the other hand might be the difficulty or even impossibility for the covalently bounded vancomycin antibiotic drugs to penetrate the protein layer formed on the implant surface shortly after implantation [23,24].

Antibiotic loaded coatings seem quite promising from the studies illustrated above, clinical applications are however not performed due to the many issues that these techniques still carry. For starters it has been reported that bacteria isolated from the implant appear resistant to the drug, also the drug susceptibility of bacteria close to the implant turned out not always to be as positive as expected. The type of antibiotic drug present in the coating influences these issues, therefore it's crucial to choose the most effective antibiotic. Furthermore, the short antibiotic release time and the restricted drug concentration released during this time limits the use of antibiotic loaded coatings in clinical applications. It has been reported that the low concentrations released by some antibiotic drug carriers doesn't exceed the inhibitory threshold. These small quantities of drug released do not contribute to bacterial death, on the contrary, they remain in the body for several years after surgery. The remnants of antibiotics present in tissues adjacent to prosthesis enhance the risk for new antibiotic resistant bacteria. It can thus be stated that there exists both an upper and lower limit for the drug release rate of ideal antibiotics delivering coatings. Drugs should be released at an effective rate for a sufficiently long period to prevent device related infections and thereafter release should decrease to prevent the development of resistant bacteria. Finally, certain types of antibiotics used in the loaded coatings may harm certain cell functions. Further investigation on their influence on tissue integration is needed in order to clinically approve the antibiotic loaded coatings on implant surface [3].

5.2 Organic antimicrobial coatings

To diminish the risk of antibiotic resistance non-antibiotic alternatives were used to fight implant related infections. Examples of those alternative antimicrobial agents are chlorhexidine, chloroxylenol and poly(hexamethylenebiguanide). The same requirements as for loaded coatings are set, namely a broad range of antimicrobial activity and a low hazard of drug resistance [3]. Chlorhexidine especially fulfils these conditions and is currently effectively used in dentistry applications such as mouth wash and gelatine treatment against periodontal infections [35]. Chlorhexidine is a biguanide positively charged compound interacting with negatively charged microbial cell surfaces. This reaction results in a destruction of the cell membrane which facilitates chlorhexidine to penetrate into the cell. The punctuation favours leakage of intracellular compounds eventually resulting in cell death [36]. This interaction occurs between microbial cells and free chlorhexidine hence release of chlorhexidine from the implant surface is required. Research showed that chlorhexidine easily absorbs to the naturally formed titanium dioxide (TiO_2) layer on titanium implants and that it detaches with the same ease. The kinetics of the adsorption and desorption depend on the surface properties such as the surface roughness and crystal structure of the formed titanium dioxide layer [3].

Incorporation of a larger number of antimicrobial agents and better release kinetics can be achieved by applying an additional coating to the titanium surface. Poly(D,L-lactic acid) indicates superior properties since this biocompatible polymer can efficiently release chlorhexidine with moderate kinetics. Besides this, the mechanical strength and hardness of this polymer contribute to its success [37]. Similar to antibiotic release coatings antimicrobial compounds can be eluted from hydroxyapatite coatings. The release kinetics however slightly differ and are characterised by a two-stage process. Firstly chlorhexidine will be released rapidly and then a moderate and sustained elution phase follows [38].

Thanks to the declined risk of bacterial resistance non-antibiotic antibacterial compounds may be utilized for a long time. This is however the only true advantage these agents have since neighbouring tissue is still prone to cell damage due to their presence. Furthermore the ideal

coating material optimising both loading content and release kinetics still hasn't been established so far [3].

5.3 Inorganic antimicrobial coatings

Inorganic antimicrobial compounds such as silver, copper and zinc may substitute the agents discussed above as they're preferred over organic compounds due to their longer lasting antibacterial effect and their stability [39]. The latter allows the integration of the compounds in the titanium coating via several processes such as physical vapour deposition, sputtering and plasma immersion ion implantation. After particle incorporation through one of the mentioned techniques bacterial attachment to the biomaterial is prohibited. In addition to restricted bacterial adhesion, growth and biofilm formation are inhibited without influencing the activity of epithelial cells and osteoblasts [3].

A well-known and efficient coating can be obtained via polymers. These can incorporate antibacterial properties through controlled release of the inorganic antibacterial compounds. The disadvantages of this technique are the limitations imposed by release kinetics which influence the release duration. Therefore, it also affects the effectiveness of the antibacterial action. A possible solution to this problem may be found in covalent immobilisation of the antibiotic molecules to the polymer. With the latter the antibacterial effect is obtained by preventing the initial adhesion of bacteria on the device coating [2].

Besides the chemical polymer coatings, physical techniques can also be used to constitute biocompatible surface layers. One of the most widely used physical techniques to produce titanium dioxide layers is plasma immersion ion implantation. The plasma state is characterised by the presence of many electrically charged or ionic particles with a tendency to colonise due to their Coulomb interactions. Via this process new ionic components can be incorporated in the surface of the original material resulting in the formation of a thin layer. Films constituted via this technique are highly favourable in orthopaedic applications due to their surface roughness which promotes osseointegration [2]. A second well known physical coating technique is physical vapour deposition where particles are transformed into their gaseous state via a physical process and then deposited on to the bulk material. A high

supersaturation of depositing atoms is obtained compared with the equilibrium pressure. At low pressure a complete and directed condensation of the atoms on the substrate is formed. Unevenly structured substrates however suffer an inhomogeneous coating. Elevated pressures may solve this problem since the directional motion of the depositing atoms will be greatly diminished by the impact with other particles. The latter technique is called sputtering [40]. Both techniques provide the advantage of bearing a great resemblance to the surface roughness and hardness of pure titanium promoting their use for load bearing implants with high (abrasive) shear forces [41].

Next to chemical and physical coating techniques also electrochemical technologies can be used. These surface modifications are based on the electric polarization of electrically conductive substrates. This can occur via three modes such as anodic oxidation, cathodic polarization or electrophoretic deposition. The main principle underlying the latter technique is the deposition of charged particles at a surface with opposite charge after local accumulation. The coagulation of the deposited particle eventually results in the formation of a coating. The main advantage of this technique is that even complex geometries can be covered by a biocompatible film [2]. During cathodic polarization a potential below the equilibrium potential is applied to deposit molecules at the cathode surface. At equilibrium electrodes flow from anode to cathode, below equilibrium however the anode will degrade slower and deposition occurs gradually inducing the opportunity to deposit hybrid layers [42].

6 Plasma electrolytic oxidation

The most optimal surface structure of the coating is micro-nano-textured. Microscale surfaces enhance osteoblast differentiation while nanoscale structures promote cell proliferation. Via electrochemical anodization an oxide coating with both these properties can be obtained on titanium implants through varying the electrolyte composition and the electrochemical parameters [43]. Micro-arc oxidation, also defined as plasma electrolytic oxidation or anodic spark deposition is an anodic oxidation process assisted by a high voltage plasma. This process is mainly used for surface modification of valve metals, these metals are characterised by their possibility to create an adherent electrically insulating anodic oxide film. Aluminium, titanium,

zirconium and tantalum are all classified as valve metals. During the oxidation the valve metal is immersed in an electrolyte solution containing dissolved salts. A different electrical potential is applied between the titanium surface serving as anode and the cathodic counter electrode. Often stainless steels are used for the latter which also serves as the reaction container. The container in which the oxidation takes place is water cooled. This is because heat will be produced during the reaction elevating the temperature of the electrolyte solution. The temperature is however an important parameter influencing the reaction kinetics therefore a constant temperature is required. The setup of this technique is illustrated below in Figure 5 [4].

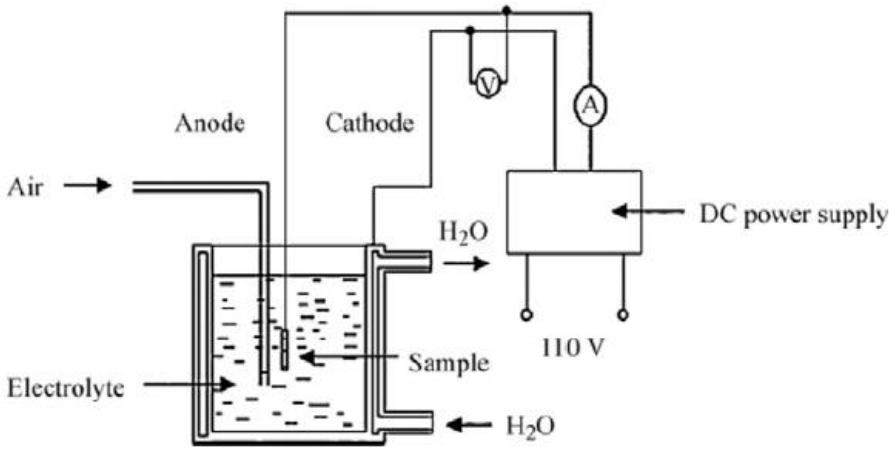

Figure 5 *- Schematic representation of the micro-arc oxidation setup [4].*

Typically, plasma electric oxidation is carried out for 5 to 180 minutes at a current density ranging between 500 and 2000 A/m² and a voltage up to 1000 V. This current can be either applied direct or alternating. During each current cycle four principal phases occur. First the voltage increases linearly in time until the breakdown voltage is reached. During this stage oxygen bubbles are released and similar to the traditional anodizing stage an oxide layer can be observed at the surface. When voltage is further increased exceeding the critical value sparks are formed due to di-electric breakdown. This breakdown colonizes current therefore breakdown takes places resulting in a local thickening of the oxide coating. Due to this thickening the coating becomes locally resistant to the increased current flow and other thinner regions become more prone to breakdown. In a similar way the oxide layer cultivates in those new breakdown areas. This phase is characterised by randomly distributed white

sparks quickly covering the entire anode surface. This alternating process of oxide formation and breakdown initiates a fluctuating cell potential. The gasification that results enables the formation of direct oxide coating which increases the total processing time. This allows the growth of the discharge sparks which transforms micro-arcs into powerful arcs. These arcs and the associated gas bubbles initiate the launch of thermal cracking of the oxide layer and which leads to the formation of large size pores. The final step gives a porous character to the coating [4].

The coating obtained via the PEO technique can be distinguished into two layers. A highly porous outer layer and a rather compact thin film below, seen as the transition layer between the bulk matrix and the porous outer layer. These two layers can be distinguished via their morphology and their chemical composition. During the oxidation process the outer layer is continuously created and destroyed by micro arcs. This process causes the growth of the porous outer layer by sequential addition of a new layer on top of another. The building material for this new layer comes from the previous sub-layer and the surrounding electrolyte. Eventually the main material for this coating creation derives from the electrolytes itself and not from the bulk elements such as aluminium in Ti6Al4V. This results in a titanium coating lacking aluminium and vanadium in its outer layer which is seen as favourable due to the decreased chance for the release of these toxic stabilisers. Plasma electrolytic oxidation parameters should therefore be optimised to a maximal potential incorporation of antibacterial compounds while limiting the concentration of toxic stabilizing elements in the outer layer [20].

6.1 Electrolyte

The electrolyte used in micro-arc oxidation can be doped with inorganic components to alter the surface properties. The components of interest are inorganic nutritious ions which play a role in mineralization, angiogenesis and homeostasis of bone tissue. They possess the capability of activating the titanium dioxide coating obtained via plasma electrolytic oxidation. The biocompatible layer hereby achieved has porous properties allowing it to be doped with inorganic components such as calcium, magnesium, phosphorous, silicon and zinc [5].

Calcium can be incorporated in the porous coating as a calcium oxide particle by using calcium acetate monohydrate electrolyte ($(CH_2COO)_2Ca.H_2O$). Calcium promotes the nucleation of apatite and the proliferation of osteoblast [5]. Promoting these processes can be done even further by also incorporating phosphorous particles in the titanium dioxide layer by adding sodium dihydrogen phosphate ($NaH_2PO_4.2H_2O$) to the electrolyte [44]. The phosphate particles will form a hydrogen phosphate group (HPO_4^{2-}) after diffusing out of the porous coating. These groups will promote the apatite induction. Simultaneous incorporation of calcium and phosphorous results in the formation of hydroxyl apatite, $Ca_2P_2O_7$ and $Ca_3(PO_4)_2$. Introduction of these phases increases the opportunity for biochemical bonding between the bone-implant interface and the bone tissue. The formation of these compounds promoting osteogenic properties is however only seen at high voltages above 450 V [5].

Besides calcium and phosphorous other compounds can be incorporated into the coating to improve the biological properties. An example of this is the addition of silicon since silicon is involved in the early stage of calcification. Furthermore is it also proven that the addition of silicon improves the adhesion of cells on the implant surface, more specifically the MC3T3-E1 cells [5]. These cells pertain to the osteoblastic cell line which implies the capacity to differentiation of the cells into osteoblasts and osteocytes, the onsets of calcified bone tissue [45]. Besides silicon also strontium can be added in the electrolyte as $Sr(CH_3COO)_2$ or $Sr(OH)_2.8H_2O$. The influence of strontium lies in its regulation function it has over the response of human fetal osteoblastic cells [5].

6.2 Antibacterial substance

The antibacterial requirements for implants are rising and stricter specification is still demanded. The main intervention after device related infections remains removal and replacement of the implant. Therefore, it is of great importance to include preventative antibacterial behaviour in the surgical intervention. Particles such as silver, copper, zinc and platinum prevent bacterial invasion and modification in nearby tissues resulting in protection against a broad spectrum of bacterial and fungal species. Nanoparticles present a greater chemical activity than the bulk material due to their high surface to volume ratio. Incorporation of these compounds can be either done by adding solid nanoparticles or by

adding a metal salt to the electrolyte solution. The disadvantage of nanoparticles is that they tend to agglomerate into clumps reducing their performance. On the other hand are pure nanoparticles more expensive than the related metal acid [46, 8].

6.2.1 Method of action

The method of action still remains unclear and the interaction mechanism also greatly depends on the bacteria it is interacting with and more specifically their cell wall composition [46]. The hypothesis verified by several studies states that the antibacterial activity lies in the adhesive interaction between the particles and the elements building up the bacterial membrane structure. The interaction causes a structural change eventually resulting in membrane degradation characterised by pit formation and cell death. Transmission electron microscopic analysis given in Figure 6, suggested that the nanoparticles not only accumulated at the exterior of the cell membrane but also penetrate into the cells resulting in a leakage of intracellular substances on its turn resulting in cell death. These mechanisms can either delay or completely inhibit bacterial growth, depending on the antibacterial content and the bacteria with which it is interacting [47].

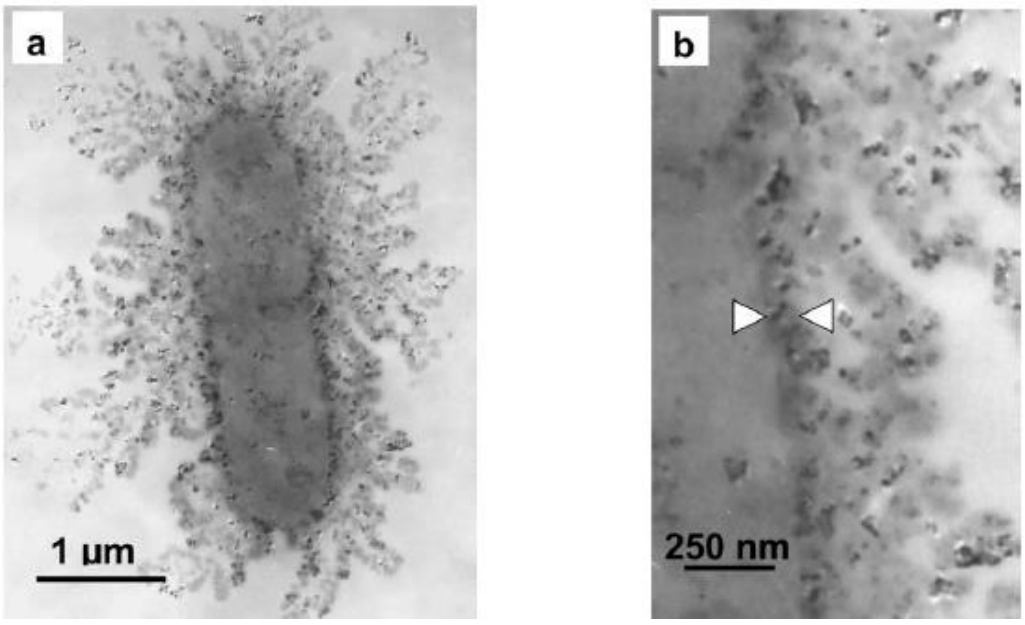

Figure 6 *- Transmission electron microscopic analysis of E. coli bacteria treated with silver nanoparticles (50 µg/cm³) over a time period of one hour. a) Entire E. coli cell. b) Magnification of the ruptured cell membrane.* [47]

Another intracellular targeting mechanism goes via the induction of reactive oxygen species (ROS) in macrophages. Here the compounds don't directly kill the bacteria but activate the macrophage itself via the synthesis of pro-inflammatory cytokines or superoxide radicals such as ROS. Oxidative stress may hereby be induced as a result of the downregulation of the transcription of oxidative stress related genes [48].

6.2.2 Silver

Silver nanoparticles are the most popular inorganic antimicrobial particles and can be incorporated into implants by direct dispersion of solid silver nanoparticles in the electrolyte during PEO. The addition has barely any effect on the morphology of the formed coating and the morphology of the silver nanoparticles is similar to that of the particles in the electrolyte [49]. After the procedure the silver nanoparticles can be found both at the surface and in the pores of the coating homogeneously distributed. Energy disperse X-ray spectroscopic analysis indicated that increasing the dose implanted in the PEO solution also increased the amount of silver nanoparticles incorporated in the coating. The presence of silver nanoparticles was confirmed by the interaction between the coated titanium sample and bacterial colonies, more specifically S. aureus colonies. Colony formation was strongly inhibited by the presence of silver with an increasing antibacterial effect for increasing nanoparticle content [46]. It has also been demonstrated that the antimicrobial activity of silver nanoparticles is higher than that of silver ions. The use of silver nanoparticles will lead to anti-bacterial effects maximized due to the increased numbers of particles per unit area. The small size of silver nanoparticles however can impose a danger to the human body since they're capable of spreading out to non-infected regions. In these environments cellular shrinkages and abnormal cell membrane shapes were observed with an increasing influence for higher silver concentrations [50].

6.2.3 Copper

Just as silver, copper is highly favourable for its antibacterial activity and low cytotoxicity. Copper can inactivate the central catabolic and biosynthetic pathways, namely catalytic clusters of dehydratases which endows copper with strong antibacterial properties [51]. Above all it has been shown that no bacteria may develop immunity towards copper, which

does occur with antibiotics [14]. Copper could be used for disease treatment in different forms ranging from copper salts and copper oxides to copper splinters, chips and nanoparticles [52]. The latter can be incorporated in titanium dioxide coatings. Their high surface to volume ratio results in greater antibacterial activity than copper due to the increased close interaction with bacterial membranes [14].

Just as silver copper may also be added as metal salt to the coating process. Copper nitrate here has an advantage over silver nitrate. Silver ions (Ag^{+}) can namely oxidize to higher valence (Ag^{2+}) and so enter the oxide coating through formation of AgO. This incorporated oxide reduces the antibacterial activity of silver. A potential solution to this problem lies in the addition of antibacterial metal oxides to the electrolyte in their highest valence state. Not silver nitrate ($AgNO_3$) but copper nitrate ($Cu(NO_3)_2$) fulfils this requirement. Energy dispersive X-ray spectroscopy confirmed the hypothesis that copper indeed is not incorporated into the formed titanium dioxide layer. The absence of these toxic ions (Cu^{2+} or Ag^{+}) on the surface of the sample greatly improve the cytocompatibility of the coating [43].

6.2.4 Zinc

Zinc oxide (ZnO) nanoparticles have proven antibacterial properties opposing enterotoxic escherichia coli (ETEC) bacteria. ZnO inhibits the adhesion of ETEC and their internalization into enterocytes [39]. Besides an interaction with the bacteria itself, the zinc oxide treatment also has an influence on the formed biofilm. Addition of zinc oxides namely resulted in a disintegrated and an intractable biofilm structure. This biofilm influence was not only seen in its growth but also in a reduced cell surface hydrophobicity easing the diffusion of the ZnO-nanoparticles through this biofilm. Both S. aureus and P. aeruginosa are biofilm generating bacteria via the synthesis of exopolysaccharides responsible for the initial adhesion and further development of the biofilm. Metal nanoparticles interfere in this exopolysaccharide synthesis [48].

This advantageous biofilm behaviour is however not seen for all bacteria [39]. Another downside limiting the use of zinc's antibacterial activity is their resemblance to antibiotics in the induction of resistant bacteria [53]. As any other antibacterial compounds, the use of ZnO-nanoparticles is also limited due to the potential cytotoxic side-effects. At the effective

bacterial dose pathogens were eliminated with no or limited (<15%) reduction in cell viability. At elevated doses however significant cell viability reduction (85%) was observed [48].

6.2.5 Gold

The interest in gold nanoparticles arose from their ease of preparation and their lower cytotoxicity compared to other nanoparticles. Their success was proven in the fight against Corynebacterium pseudotuberculosis, a bacterium mainly affecting sheep and goats. Animals infected with this bacterium are difficult to treat with antibiotics due to the thick capsule surrounding the abscesses. High resolution electron microscopic analysis indicated the morphological changes of bacterial cells indicating the penetration of these gold nanoparticles through the cell membrane and gold aggregation in the cytoplasm [54]. Both the method of action and the efficiency of these antibacterial gold nanoparticles depend on their preparation method influencing size and surface modifications [55].

7 Objective of the thesis

Within this master thesis, plasma electrolytic oxidation processes will be used to deposit a porous titanium dioxide coating onto titanium substrates. Antibacterial properties will be added to the TiO_2 coating by incorporating anti-bacterial elements such as copper or silver salts into the electrolyte. The porous nature of the anodized films enhances the anchorage of the implants and also increase the release of the incorporated anti-bacterial agents around the titanium implants. Furthermore, biocompatibility of the layer will be increased via the incorporation of calcium and phosphorous, forming a hydroxyapatite-like coating

Process parameters such as voltage, deposition time, electrolyte concentration etc. will be varied in the synthesis and their effect on the deposited coating's characteristics will be studied. Physical and chemical characteristics of the deposited coating will be studied using different characterization techniques. In addition, anti-bacterial tests and cell tests will be performed on the developed coatings to study the anti-bacterial performance and the cytotoxicity of the developed coatings. Mechanical tests will be performed to establish the performance of the coating in medical implant applications.

8 Sample preparation

8.1 Grinding and polishing

Commercially pure titanium discs, 12 mm in diameter and 3 mm in thickness purchased from L&D Techniek NV were used as substrates. Prior to the treatment, the samples were grounded with SiC paper from 320 up to 1200, mirror-like polished with diamond paste and then ultrasonically cleaned with acetone, ethanol and distilled water each for one hour.

8.2 PEO

For the coating process the set-up illustrated in Figure 7 was used. The titanium samples were subjected to PEO using calcium ($Ca_5(PO_4)_3OH$) and phosphorous (NaH_2PO_4-$2H_2O$) along with silver ($AgOOCCH_3$) or copper ($Cu(OOCCH_3)_2$) salts as an electrolyte at a voltage of 450 V for 5 minutes. The stainless-steel holder was cooled via a controlled temperature of 10 °C using an external water cooling system to maintain a constant temperature during the treatment. The maximal applied current was limited to 1 A.

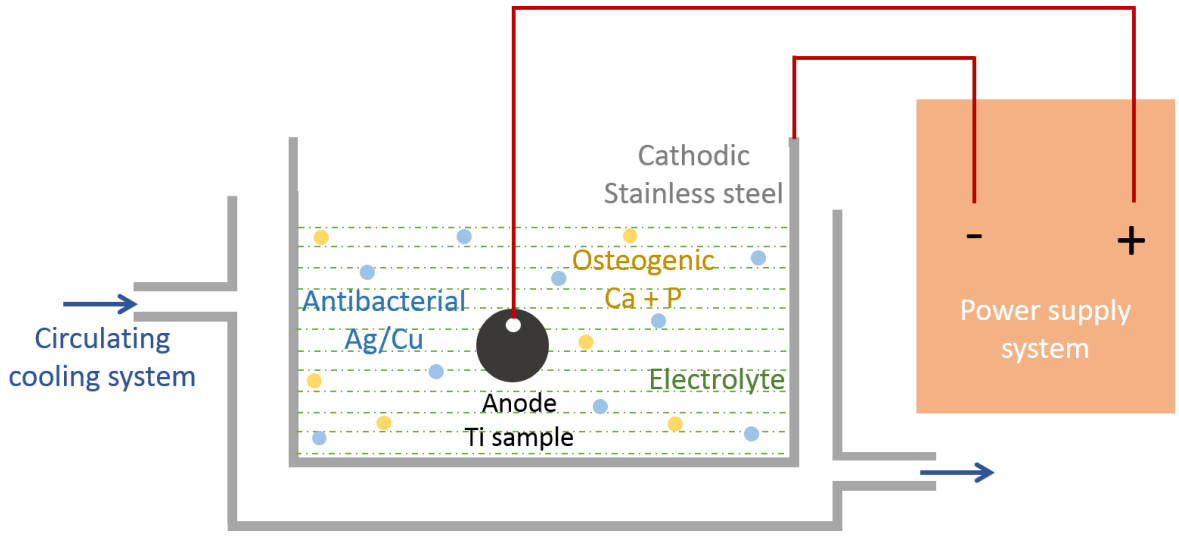

Figure 7 *- Schematic representation of the used PEO set-up.*

9 Sample Characterization

9.1 X-ray photoelectron spectroscopy (XPS)

The chemical composition of treated titanium samples is investigated by x-ray photoelectron spectroscopy (XPS), which is performed on a PHI 5000 Versaprobe II spectrometer employing a monochromatic aluminum Kα X-ray source (hv=1486.6 eV) operating at 43,5 V resulting in a beam size of 100 µm. During the analysis, the pressure in the chamber is maintained at 10^{-6} Pa or lower and the photoelectrons were detected with a hemispherical analyzer positioned at an angle of 45^{o} with respect to the normal of the sample surface. Survey scans and individual high spectra of titanium (Ti 2p), oxygen (O 1s), carbon (C 1s), phosphorous (P 2p), calcium (Ca 2p) and silver (Ag 3d) or copper (Cu 2p3) were recorded with a pass energy of 187,85 eV and 23,5 V. On each sample surface 4 spots were selected for measurements. The elements present on treated titanium samples were identified and quantified from XPS data suing Multipak software (Version 9.6.2).

9.2 Scanning electron microscopy (SEM) – energy dispersive X-ray spectroscopy (EDX)

Surface and cross-section morphology and chemical composition of the titanium dioxide layers were analyzed using the following scanning electron microscopes JSM-6010 PLUS/LV, JEOL & JSM-7600F FEG, JEOL. The microscope was operated under an accelerating voltage of 7 kV and a working distance of 11 mm.

9.3 Atomic force microscopy (AFM)

Changes in surface topography were quantified using an XE-70 AFM system (Park Systems™, Suwon, South Korea). Micrographs measuring 15 × 15 µm² were recorded in non-contact mode using a silicon-based cantilever (Nanosensors™ PPP-NCHR, Neuchâtel, Switzerland). Micrographs were analyzed using the included XEP processing software (Version 1.8.0) and were subjected to an X–Y plane autofit procedure prior to roughness determination. In this

study, for each sample, measurements were done on three random locations and the sample roughness given is the average of the three obtained values.

9.4 Inductively coupled plasma mass spectroscopy (ICP-MS)

The silver ion release kinetics were monitored by NexION 350 ICP-MS (PerkinElmer, Massachusetts, USA). The silver doped titanium dioxide deposited discs were immersed into 20 ml of distilled water in small bottles at an elevated temperature of 37 °C to mimic in vivo conditions for different time periods (6 hours, 1 day, 3 days, 5 days and 7 days). The concentration of released silver in water was determined by using a NexION 350 ICP-MS system.

9.5 Anti-bacterial test

E. coli ATCC 25922 and S. aureus ATCC 6538 were grown on LB agar or in LB broth at 37 °C. An overnight culture was standardized to optical density (at 590 nm) of 0,05 and subsequently diluted 1:1000 in 2% LB broth. 2 ml of the resulting suspension was added to the wells of a 12-well microtiter plate, each well contained one sample. Microtiterplates were subsequently incubated at 37 °C for 24 hours, while shaking (100 rpm). After 24h, samples were removed from the microtiterplates and placed in 10 ml physiological saline (0.9% NaCl) after which they were vortexed and sonicated in order to remove all surface-attached bacteria from the samples. Serial dilutions of the resulting suspension were used to determine the number of colony forming units (CFU) by plating on LB agar. Experiments were performed in 4 independent samples (n=4). Data are represented as a mean with standard deviation.

9.6 Cytotoxicity test

9.6.1 Cell culture

PEO treated and untreated polished titanium substrates were sterilized by exposure to UV light (Sylvania; 254 nm wavelength) for 30 minutes. Samples were placed in a 24-well plate. MC3T3 cells were seeded onto the samples at a density of 50,000 cells/ml of medium, using a total of 1 ml of medium. Cell culture was performed using a DMEM glutamax medium (Gibco

Invitrogen) enriched with 15% fetal calf serum (Gibco Invitrogen), 2 mM L-glutamine (Sigma-Aldrich), 10 U/ml penicillin, 10 mg/ml streptomycin and 100 mM sodium-pyruvate (all from Gibco Invitrogen). The cultures were incubated at 37 °C under 5% CO_2 for 1 day and 7 days which is the characteristic time required for human foreskin fibroblasts to adhere and proliferate on surfaces. Cell adhesion, proliferation and viability were measured for 7 days and tissue culture polystyrene plates (TCPS) were used as a positive control.

9.6.2 Live and dead immune fluorescence microscopy

Live-dead cell staining was used to evaluate cell viability. After 1 day and 7 days of seeding, the cells were incubated in 2 µl (1 mg/ml) of calcein-AM and 2 µl (1mg/ml) of propidium iodide in 1 ml PBS (phosphate-buffered saline) for 10 minutes at room temperature, rinsed twice with PBS solution and then imaged with a fluorescence microscope (Olympus; IX 81), using the appropriate filters.

9.6.3 MTT assay

Cell response to the treated and untreated titanium substrates was assessed by cell proliferation and viability (mitochondrial activity). Cell viability was measured after 1 day and 7 days of MC3T3 culture by replacing the culture medium by 0,5 ml (0,5 mg/ml) 3-[4,5-dimethylthiazol-2-yl]-2,5-diphenyl tetrazolium bromide (MTT) reagent. The samples were incubated at 37 °C at 5% CO_2 for 4 h in MTT solution. Mitochondrial dehydrogenase enzymes of viable cells reduced the tetrazolium ring to purple formazan crystals. The formazan crystals were dissolved in a lysis buffer (1% Triton-X100 in isopropanol/ 0.04 N HCl) for 30 min, then 200 µl of this solution was transferred to a 96-well plate and the optical density (OD) was measured at 580 nm using a spectrophotometer (BioTek; USA). Background absorbance at 750 nm was subtracted from the measured absorbance.

9.6.4 Cell fixation for SEM analysis

The titanium disks were gently removed from the culture media and rinsed 3 times with PBS to remove non-adhered cells. The cells were then fixed in a fixing solution (2,5% glutaraldehyde with cacodylate buffer) for 1 h, washed in a buffer solution (fixing solution

without glutaraldehyde) and then dehydrated in increasing concentrations of ethanol (50%, 75%, 85%, 95% and 100%) for 10 minutes each. After dehydration, the titanium disks were immersed in hexamethyldisilazane (HMDS) twice for 10 minutes and air-dried.

9.7 Scratch test

Tribology analysis was performed to evaluate the mechanical properties of the porous titanium dioxide layer since the coating should possess sufficient wear resistance to prevent the release of debris in the body. To perform these tests the pin-on-disk small scale tribometer (PoD ASTM G132) shown in Figure 8 was used. A steel indenter with a diameter of 8 mm was used while held at an initial arm position of 85 mm. The device was operated at the minimal sliding speed of 3 mm/s following a circular sliding path. The load applied on the sample through the pin was varied between 1 N and 10 N. During all tests the same indenter was used, possibly influencing the results, as the intender shape might have changed due to damage caused by previous tests.

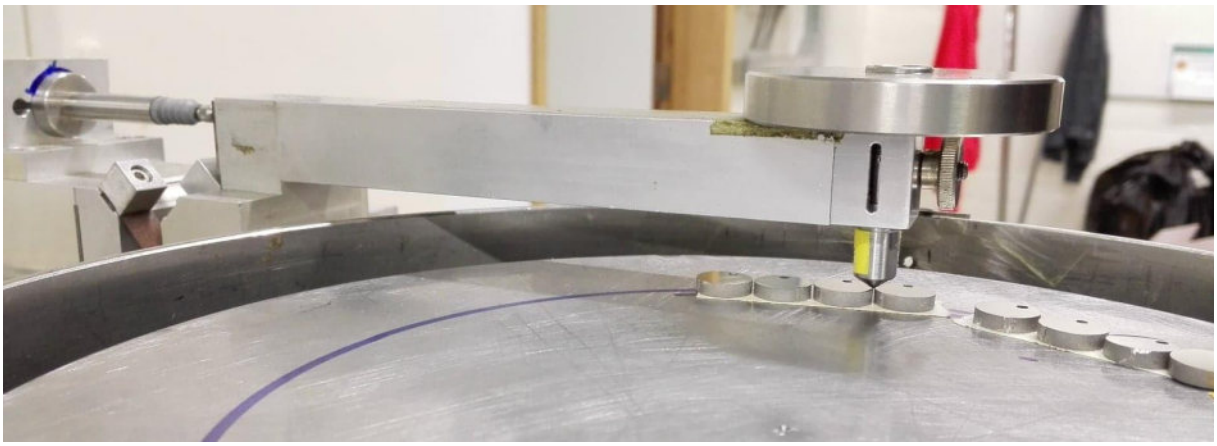

Figure 8 *- Picture of the pin on disk tribology machine used for mechanical testing. Device code PoD ASTM G132 PO/047 EQ001141.*

Results and discussion

10 PEO parameters

The plasma electrolytic oxidation parameters were optimised in order to obtain a porous titanium dioxide layer mimicking hydroxyapatite's ($Ca_5(PO_4)_3OH$) morphology and composition to promote osteogenic properties while containing antibacterial particles. Optimal osteogenic conditions were obtained with a calcium over phosphate ratio above 1 with an optimal of 1,67 which is the case for hydroxyapatite. To obtain this ratio sodium dihydrogen phosphate-dihydrate (NaH_2PO_4-$2H_2O$) and calcium acetate monohydrate ($Ca(OOCCH_3)_2$-H_2O) were added to the base electrolyte with the respective concentrations of 2 g/L and 5 g/L. Antibacterial properties on their turn were obtained through the addition of silver acetate ($AgOOCCH_3$) or copper acetate ($Cu(OOCCH_3)_2$) with a varying concentration ranging between 0,1 g/L and 1 g/L.

For the oxidation, pure polished titanium samples were subjected to a plasma electrolyte oxidation process for 5 minutes at a voltage of 450 V. During the process voltage gradually increases to 300 V, which is the minimal needed voltage to obtain plasma and further to 450 V after which the voltage maintained constant. Current density on the other hand started to increase and maintained constant and then gradually decreases once the maximal voltage is reached. This process is illustrated below in Figure 9 and Figure 10.

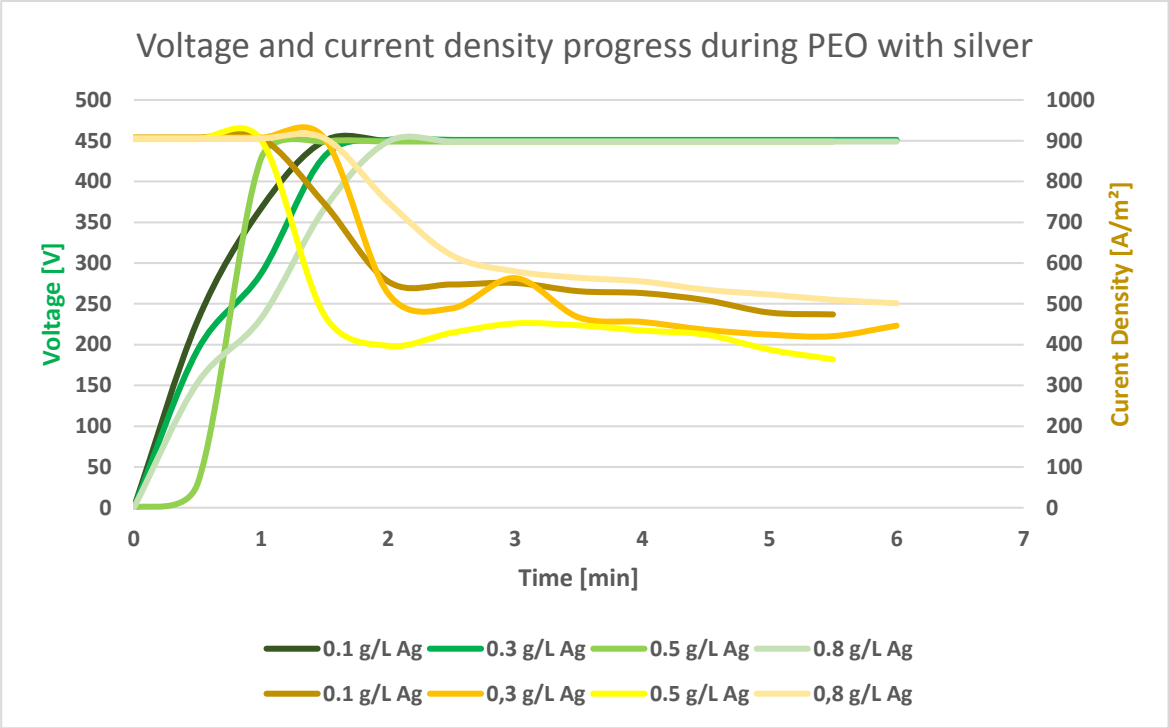

Figure 9 *- Voltage and current density evolution during the PEO process with the silver doped electrolyte.*

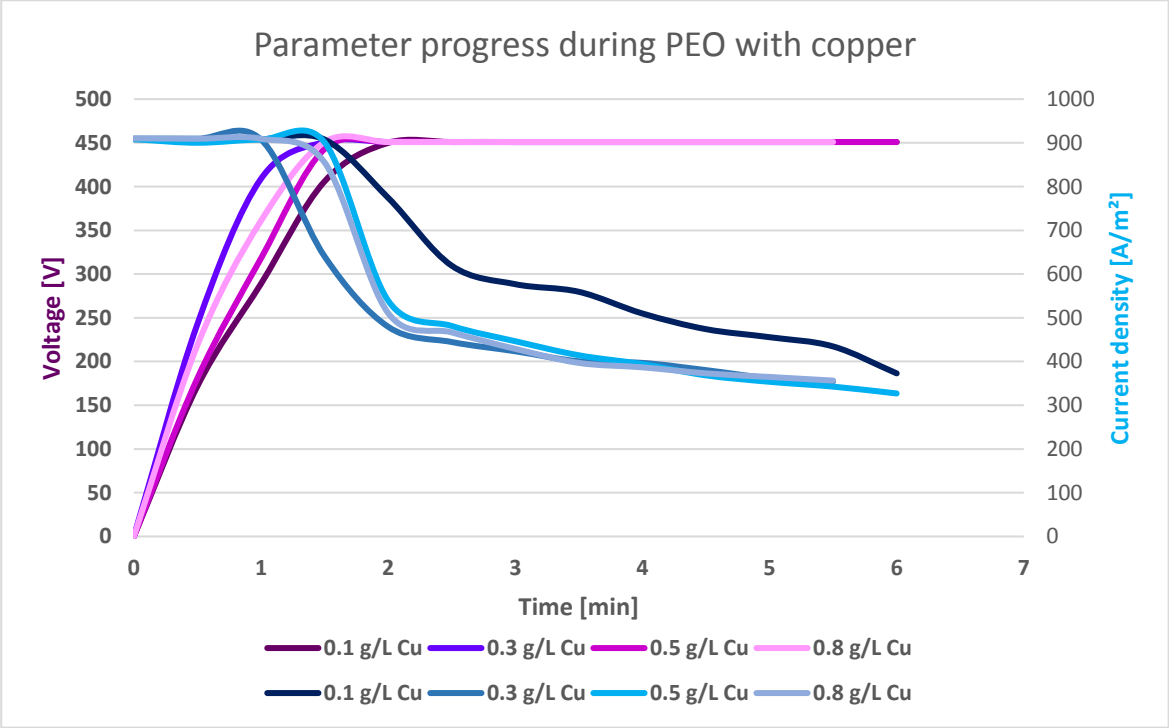

Figure 10 *- Voltage and current density evolution during the PEO process with the copper doped electrolyte.*

Both the voltage and the current density follow a similar pattern despite the conditions of the electrolyte. The electrolyte concentration or the type of the electrolyte does not greatly influence the process parameters as can be seen in Figure 11 and Figure 12.

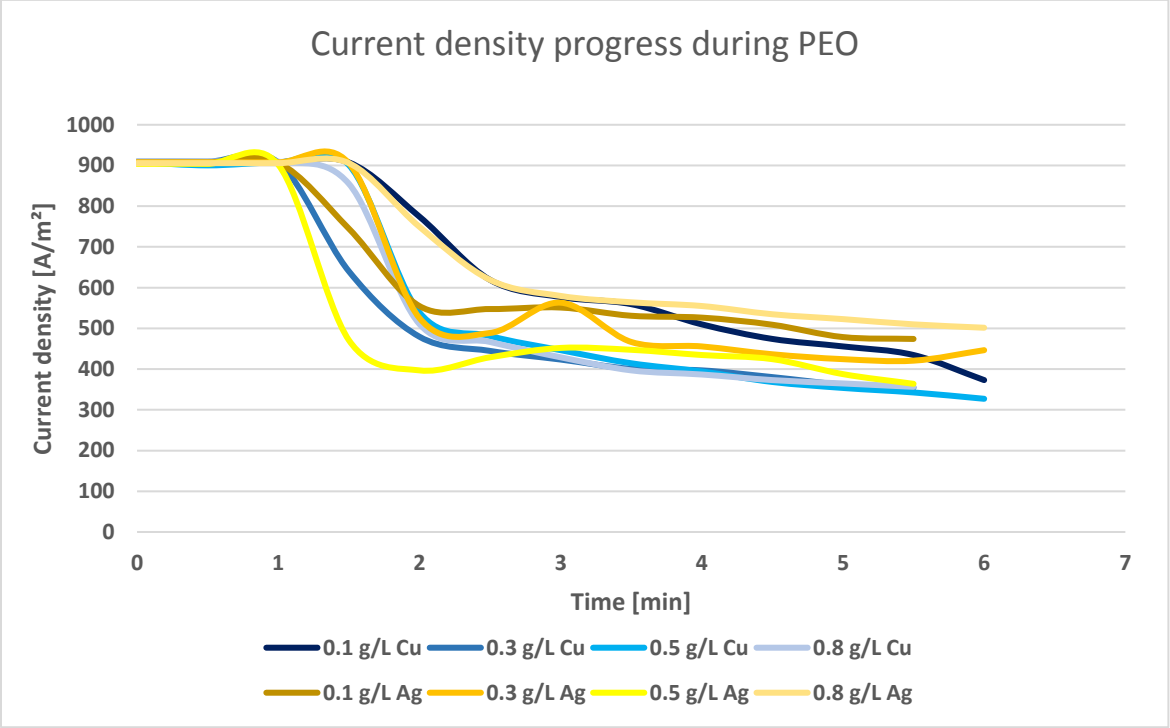

Figure 11 *- Comparison of the current density evolution during the PEO process of the copper and silver doped electrolyte.*

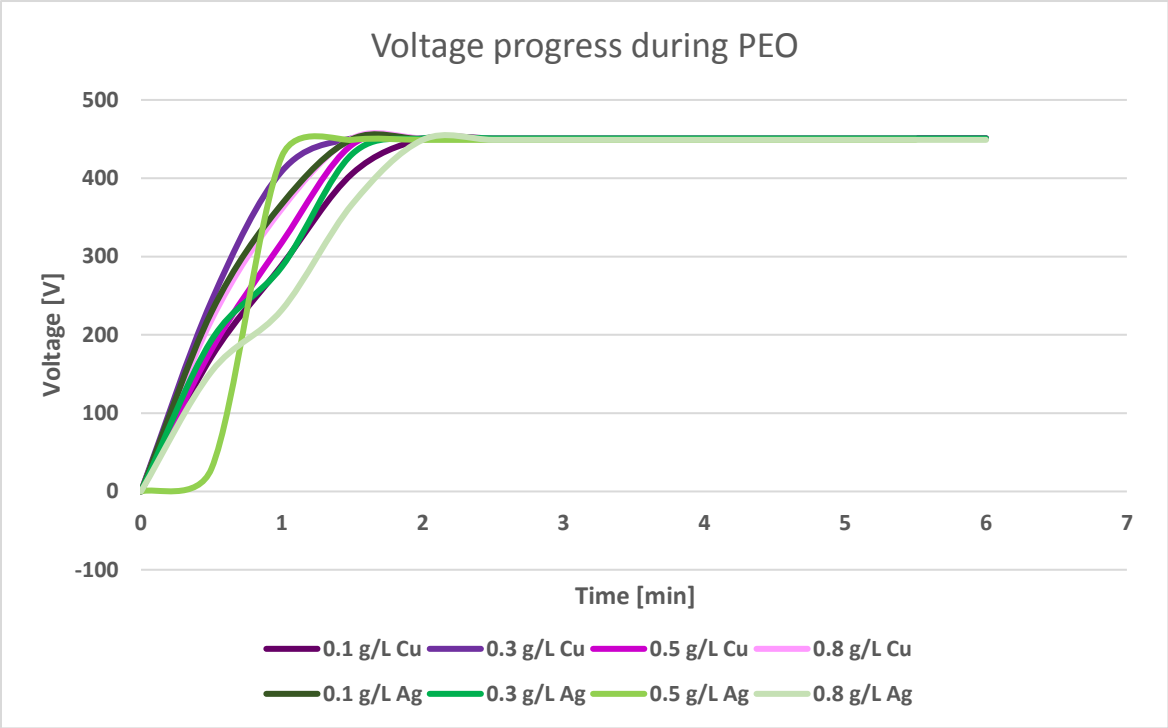

Figure 12 *- Comparison of the voltage evolution during the PEO process of the copper and silver doped electrolyte.*

11 XPS

As mentioned before silver or copper were added to the electrolyte for antibacterial properties and calcium and phosphorous were added to promote osteogenic properties and reduce cytotoxicity. Calcium phosphate is a ceramic material proven to support bone apposition to enhance osteoconduction and accelerate healing processes. In order to fabricate a hydroxyapatite like coating a calcium to phosphorous ratio of about 1,67 has to be attained. Several electrolyte concentrations were used to perform plasma electrolyte oxidation with the purpose of attaining the required Ca/P ratio after which the composition of the deposited oxide layer was determined with X-ray photoelectron spectroscopy, the results are given below in Table 1. As a stable voltage and current density is required to obtain plasma a compromise had to be made regarding the calcium to phosphorous ratio. Electrolyte concentrations that reached the needed current and voltage for the formation of the titanium dioxide layer didn't contain enough calcium to attain the required ration. A ratio above 1 was chosen as sufficient to promote osteogenic properties to a certain amount without mimicking the actual bone composition.

X-ray photoelectron spectroscopy furthermore also indicated that an increased silver concentration in the electrolyte results in a greater silver concentration in the titanium dioxide layer. From XPS however no information can be obtained about the location in the pores and the homogeneity of the distribution of these silver particles.

Table 1 *- XPS analysis of the TiO_2 layer obtained after PEO from the silver doped electrolyte with varying electrolyte compositions.*

$Ca(OOCCH_3)_2 \bullet H_2O$ [g/L]	**NaH_2PO_4 [g/L]**	**$AgOOCCH_3$ [g/L]**	**Ca/P [-]**	**Ag [at%]**
4	2,7	0,8	0,581 ± 0,365	1,94 ± 0,30
4,5	2,7	0,8	0,523 ± 0,585	1,69 ± 0,27
5	2,7	0,8	0,436 ± 0,225	1,11 ± 0,05
5	**2**	**0,8**	**1,23 ± 0,925**	**1,56 ± 0,10**
5	**2**	**0,5**	**1,35 ± 1,30**	**1,10 ± 0,41**
5	**2**	**0,3**	**1,09 ± 0,530**	**0,74 ± 0,05**
5	**2**	**0,1**	**1,57 ± 0,345**	**0,44 ± 0,09**
5	1	0,8	0,678 ± 0,290	2,07 ± 0,12
5	1	0,3	0,569 ± 0,305	1,24 ± 0,11
5	1	0,1	0,581 ± 0,655	0,41 ± 0,06

Next to silver acetate copper acetate can be added to the electrolyte as antibacterial component. Literature suggests an electrolyte concentration with a molar copper to phosphorous ratio of 0,21 [56]. Maintaining the same calcium acetate and sodium monohydrate conditions results in a copper acetate concentration of 0,636 g/L which lies in the same range as the used silver electrolyte composition. Therefore, the same concentrations were chosen and analysed with XPS. Despite the fructuous Ca/P ratio seen with these conditions in a silver doped titanium dioxide layer, the one obtained from copper conditions isn't sufficient to optimally promote osteogenic properties. Finally, an increase in copper atomic percentage was seen for increasing electrolyte concentrations.

Table 2 *- XPS analysis of the TiO_2 layer obtained after PEO from the copper doped electrolyte with varying electrolyte compositions.*

$Ca(OOCCH_3)_2 \bullet H_2O$ [g/L]	**NaH_2PO_4 [g/L]**	**$C_4H_6O_4Cu$ [g/L]**	**Ca/P [-]**	**Cu [at%]**
5	2	0,1	0,650 ± 2,66	1,26 ± 1,07
5	2	0,3	0,548 ± 1,52	1,21 ± 1,09
5	2	0,5	0,492 ± 0,485	2,90 ± 1,57
5	2	0,8	0,521 ± 0,195	3,93 ± 0,79

The XPS survey spectra of the silver doped coating can be seen in Figure 13 and that of the copper doped coating in Figure 14. For increasing concentrations of the antibacterial particle (Ag/Cu) in the electrolyte an increase of the peak at the binding energy of the associated particle is seen. A more detailed spectrum of this silver and copper peak is provided in Figure 15.

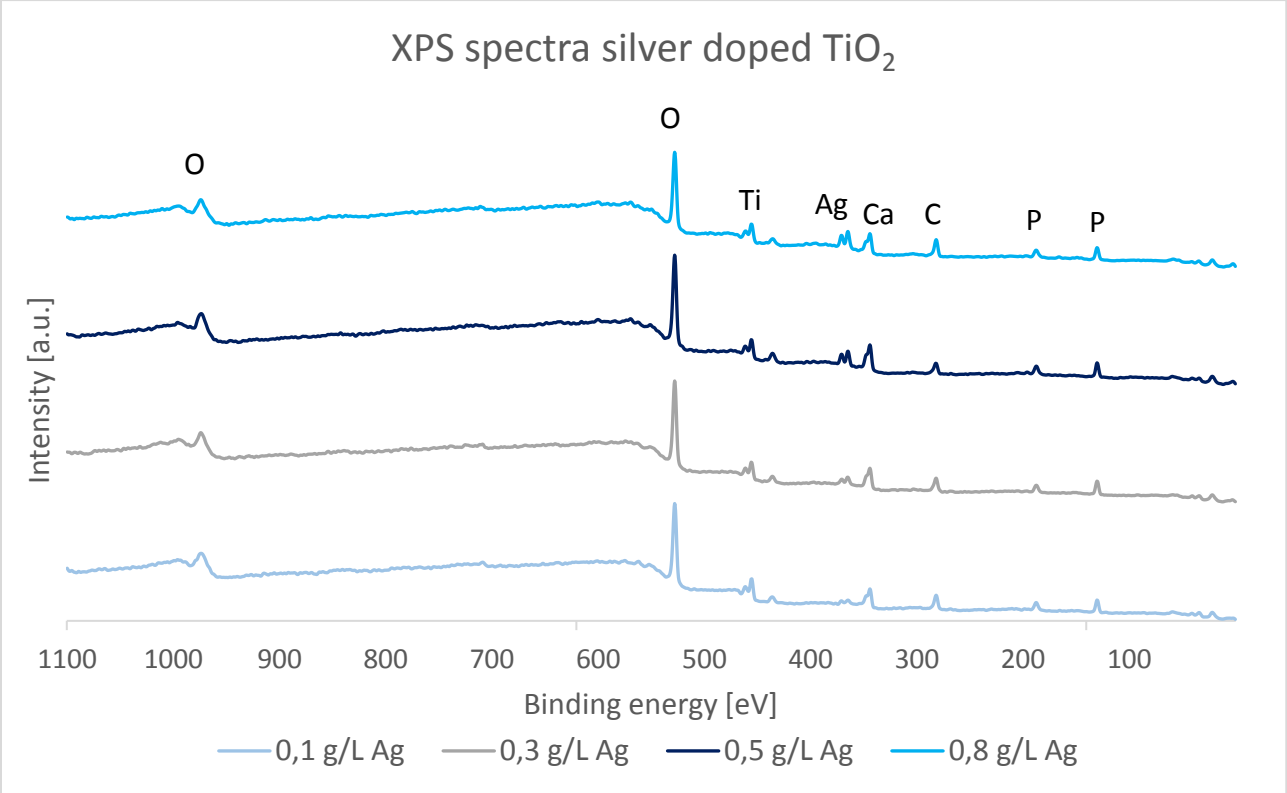

Figure 13 *- XPS spectra of the silver doped layer. An increase of the peak around 370 eV is seen for increasing silver concentrations.*

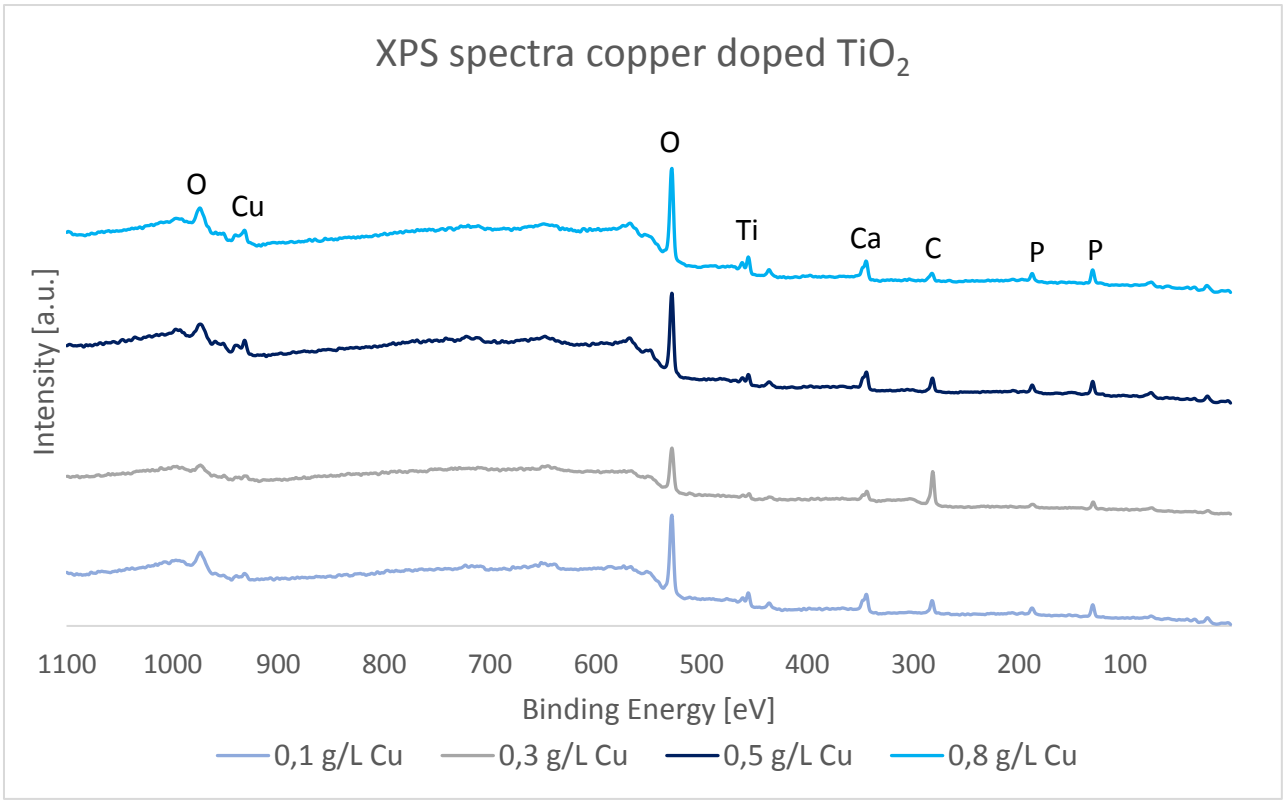

Figure 14 *- XPS spectra of the copper doped layer. An increase of the peak around 950 eV is seen for increasing copper concentrations.*

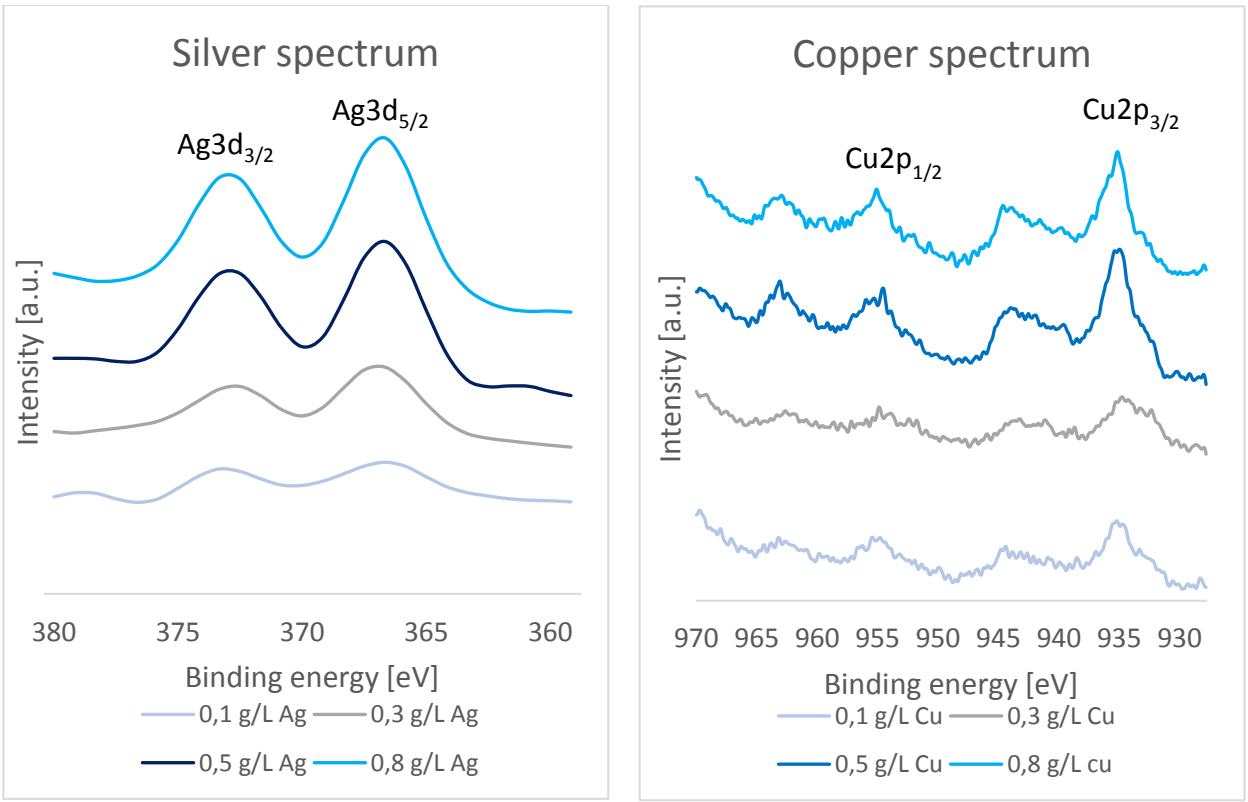

Figure 15 *- Detailed spectra of the peak increase at the binding energy of the antibacterial particles. Left: Silver doped TiO_2. Right: Copper doped TiO_2.*

12 SEM – EDX

Scanning electron microscopy was performed on all samples to compare the morphology of the titanium dioxide layer obtained with plasma electrolyte oxidation with a calcium phosphate layer deposited through other techniques. Figure 16 illustrates pure hydroxyapatite coatings on titanium samples obtained via sol-gel method and thermal spray technique. In both cases the coating is dense, uniform and porous. These characteristics can also be seen in the SEM images of the titanium dioxide layer obtained via PEO containing calcium and phosphorous, as given in Figure 17 and Figure 19.

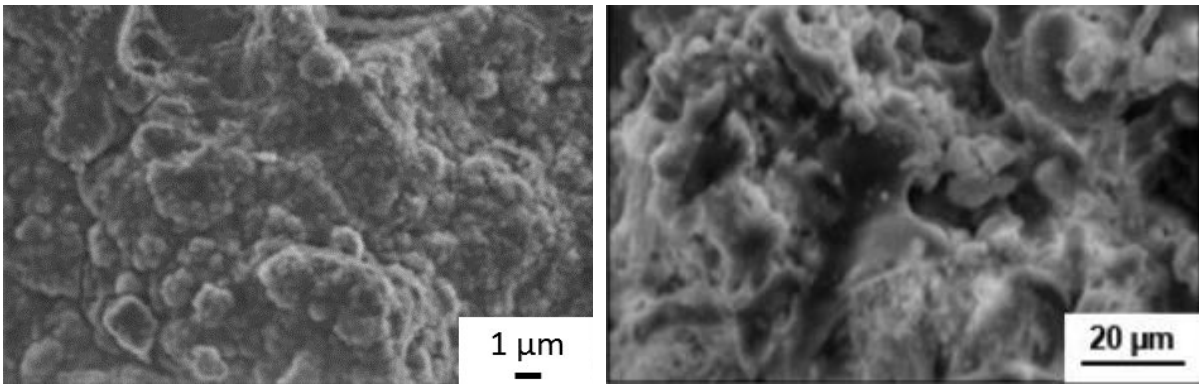

Figure 16 *- Hydroxyapatite coating on bulk titanium dioxide. Left: Deposited calcium phosphate via sol-gel method. Right: Hydroxyapatite coating via stand-off distance thermal spray technique.*

Furthermore, the SEM images can give an indication of the layer porosity which may have an influence on the release rate of the antibacterial particles. From Figure 17 and Figure 19 it can be seen that the concentration of the metallic salt has no influence on the surface morphology. All conditions result in a porous layer, both micro and nanoscopic.

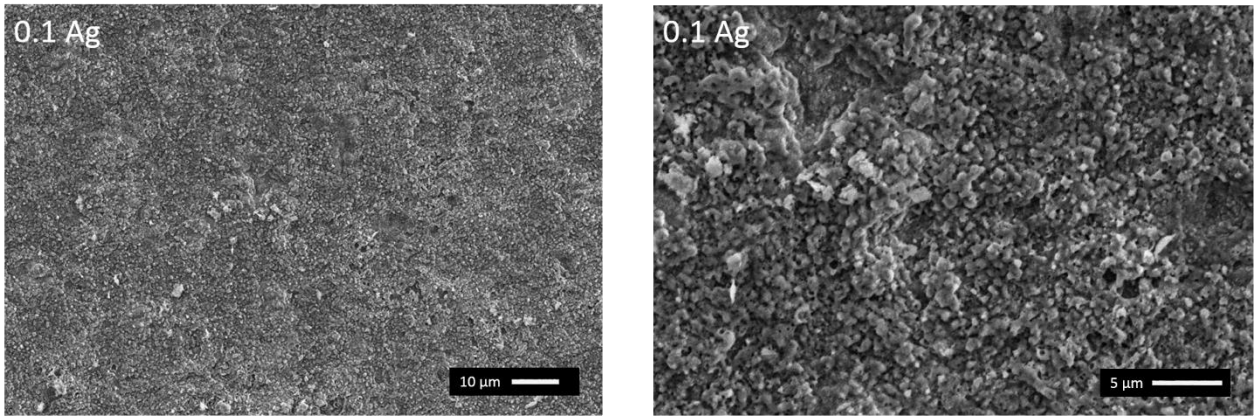

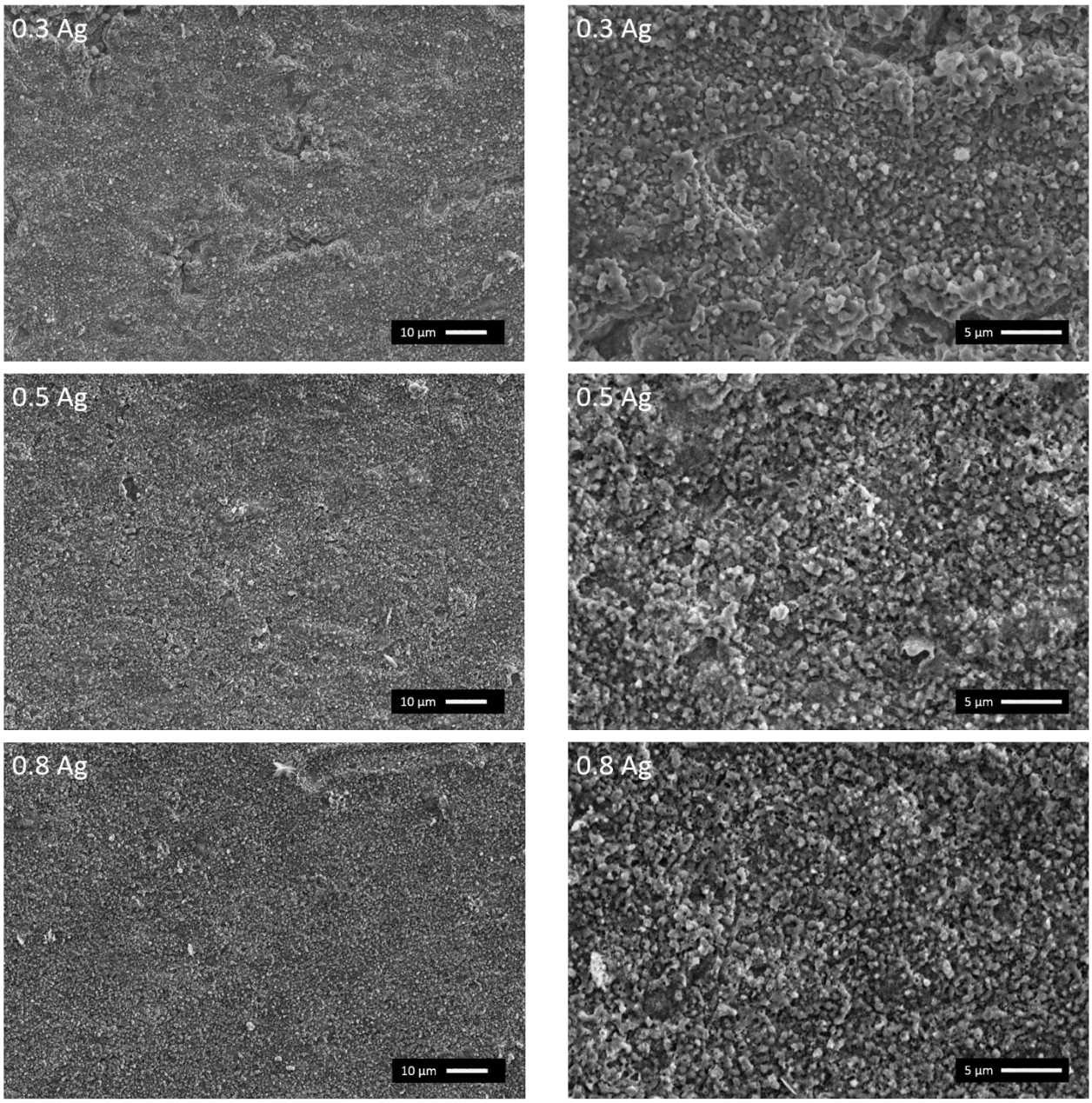

Figure 17 *- SEM images of the titanium dioxide layer containing different silver concentrations. Left: Magnification 1000x. Right: Magnification 3000x.*

In addition, stability of the prepared coating on titanium was observed by immersing the sample in distilled water for several days in a shaking bath at a temperature of 37 °C. SEM images of the samples were obtained after immersion for 17 days. From Figure 18, it can be seen that the morphology of the coating did not change after water immersion. Overall no difference in porosity and surface structure can be seen. Hence, it can be concluded that the layer properties are preserved even after contact with the aqueous medium which will be the case under in vivo conditions.

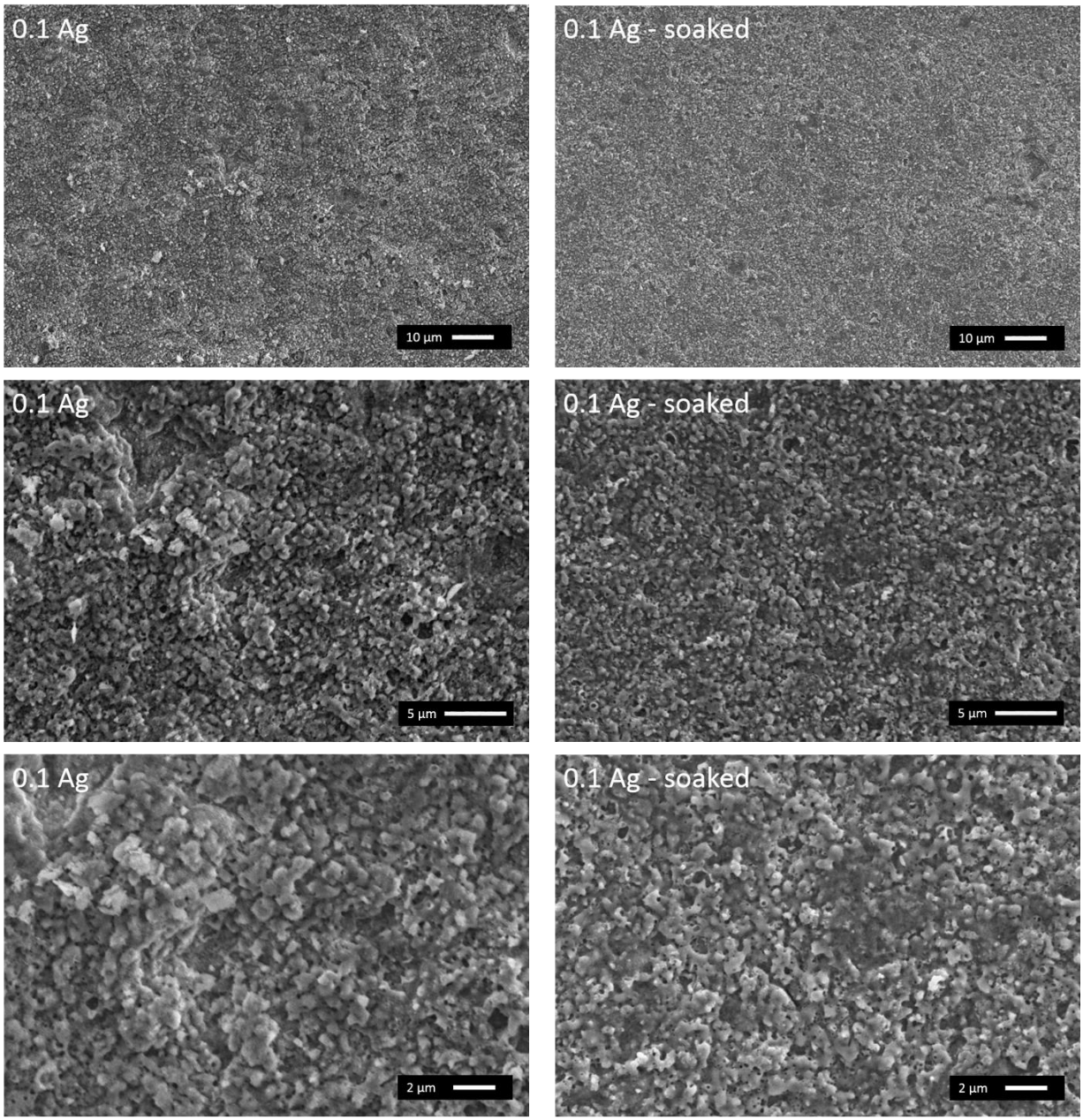

Figure 18 *- SEM images illustrating the influence on the TiO_2 layer of drainage in distilled water at 37°C. Top: Magnification 1000x. Middle: Magnification 3000x. Bottom: Magnification 5000x.*

Substitution of the antibacterial particles barely influences the surface morphology as can be seen in the SEM images in Figure 19. The porosity of the copper doped titanium dioxide layer is comparable to the one containing silver, while the overall morphology is slightly altered resulting in a greater microscopic layer variation when copper acetate was added to the electrolyte. It can however not be fully concluded that this influence is purely caused by the copper particles and not by somewhat altered process conditions.

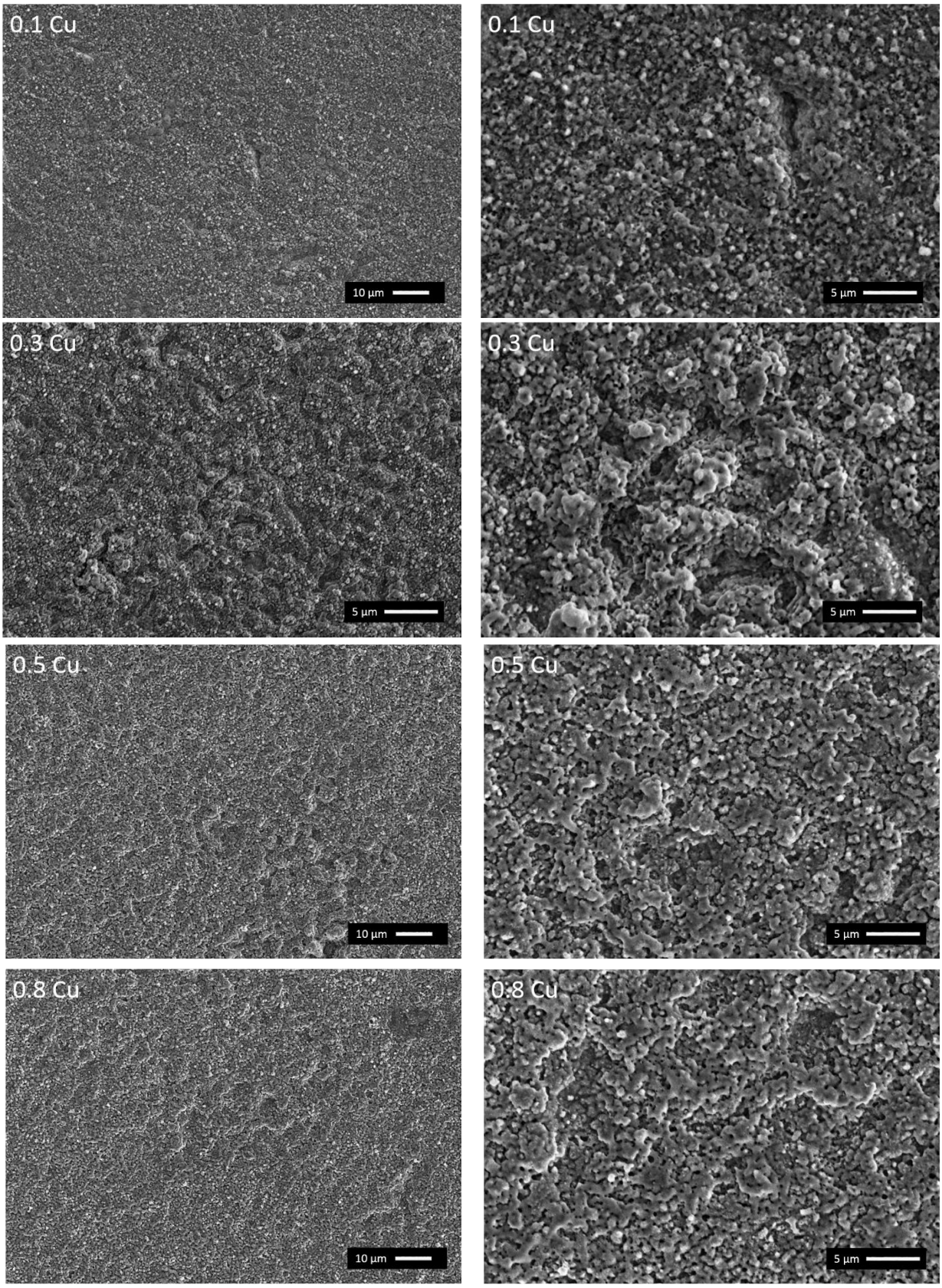

Figure 19 *- SEM images of the titanium dioxide layer containing different copper concentrations. Left: Magnification 1000x. Right: Magnification 3000x.*

Scanning electron microscopy allows the analysis of secondary electrons and backscattered electrons. Secondary electrons are created after inelastic collision of the primary electron and the atom. An outer shell atom with restricted energy is hereby excited close to the surface. From the detected intensity of these surface electrons a topographic image of the sample can be obtained. Backscattered electrons on the other hand are formed due to a deflection of the primary electron caused by an interaction with the atom nucleus. This elastic collision barely reduced the energy of the incoming electron wherefore electrons with a greater energy can be detected. The intensity is related to the sizes of the atoms which allows the detection of different material phases. Atoms with a greater atomic number possess a greater surface resulting in more back scattered electrons and light images. Backscattered analysis was therefore used to detect the heavier antibacterial silver and copper atoms as they appear lighter.

Figure 20 and Figure 21 illustrate the presence of non-agglomerated silver and copper elements in the porous titanium dioxide layer. Furthermore, it illustrates the more or less homogeneous distribution of the antibacterial particles over the width and the depth of the layer. The particle clustering and distribution appeared independent of its electrolyte concentration. The larger magnification of these images also indicates the range of porosity and the housing of the silver or copper atoms in these pores.

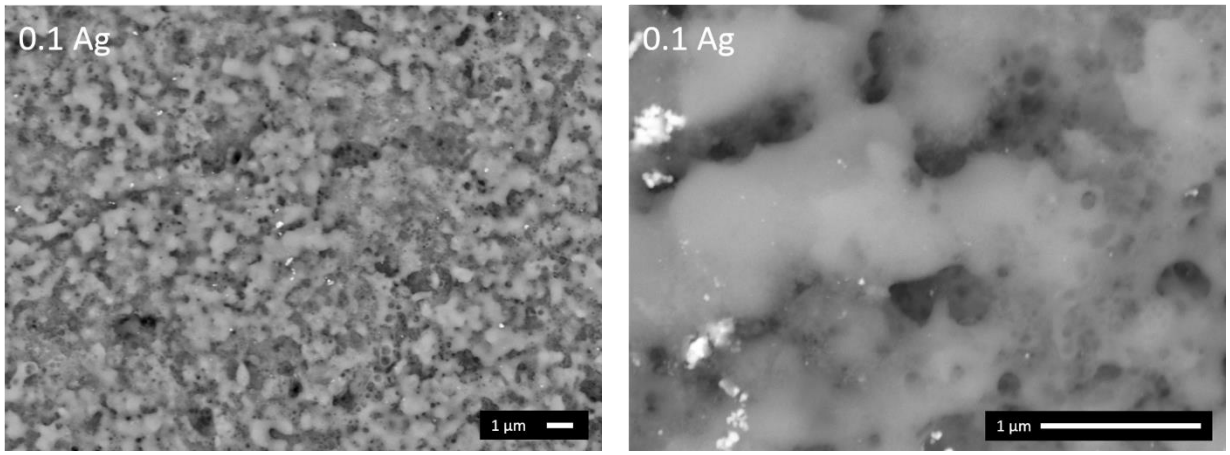

Figure 20 *- Backscattered electron SEM images enlighten the heavier silver particles in the titanium dioxide layer. Left: Magnification 5000x. Right: Magnification 30000x.*

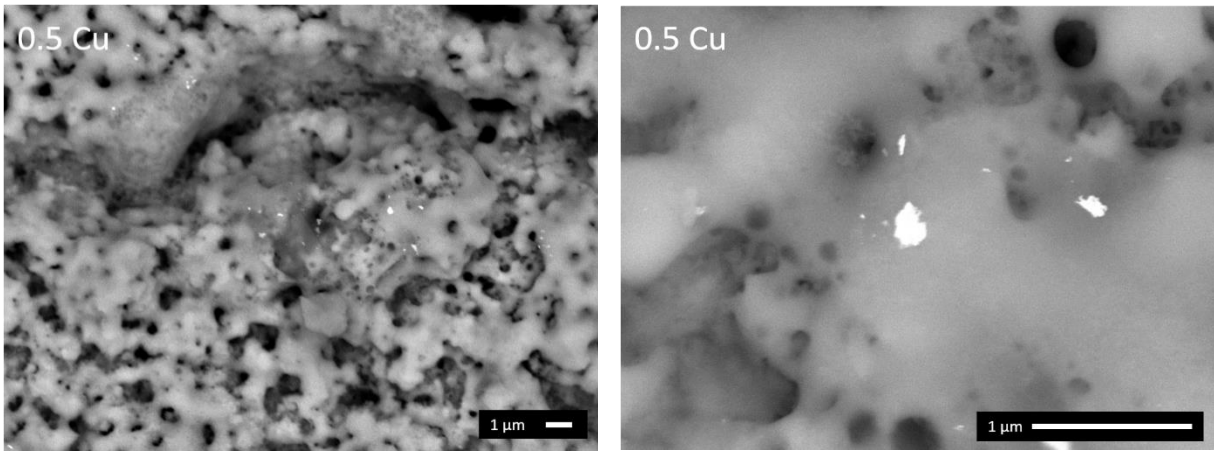

Figure 21 *- Backscattered electron SEM images enlighten the heavier copper particles in the titanium dioxide layer. Left: Magnification 5000x. Right: Magnification 30000x.*

Energy dispersive X-ray analysis was used besides XPS to determine the chemical composition of the antibacterial titanium dioxide layer. The technique is in a certain manner analogous to X-ray photoelectron spectroscopy. The depth of analysis however differs as XPS is a surface technique restricted to the upper layer of approximately 5 nm while EDX allows the analysis of a few micro meters representing the 'bulk' concentration [57]. Furthermore EDX is rather used for point or line analysis while XPS provides an average chemical composition of the entire surface. The EDX data of several mapping areas was used to calculate the average layer composition, the results are given below in Table 3 and Table 4.

When comparing the surface EDX data with the XPS data a smaller calcium to phosphorous ratio is observed in EDX, promoting osteogenic properties less optimal. This can be explained by the different principle underlying these techniques, suggesting that the phosphorous particles can be found closer to the bulk in the titanium dioxide layer while calcium is present at the surface, easing their detection through XPS analysis.

Moreover, it can also be observed that both copper and silver atomic percentage obtained from EDX is much less than that of the XPS. The increasing trend of the electrolyte concentration are also not followed in the EDX data. Both deviations can be explained by the inhomogeneity of the particle distribution at greater depth therefore it is possible that the selected spots are underrepresented regarding these elements.

Table 3 *- Energy dispersive X-ray surface analysis of the obtained silver doped titanium dioxide layer under varying conditions. Calculated calcium over phosphorous ratio for the measured atomic percentages.*

Condition	Ti [at %]	O [at %]	Ca [at %]	P [at %]	Ag [at %]	Ca/P [-]
0.1 g/L Ag	28,53 ± 0,3	67,50 ± 0,3	0,37 ± 0,0	3,50 ± 0,1	0,043 ± 0,1	0,104
0.3 g/L Ag	28,86 ± 0,2	65,85 ± 0,2	0,30 ± 0,0	3,80 ± 0,1	0,19 ± 0,1	0,078
0.5 g/L Ag	30,32 ± 0,2	65,47 ± 0,2	0,21 ± 0,0	3,63 ± 0,0	0,19 ± 0,1	0,058
0.8 g/L Ag	29,74 ± 0,1	66,88 ± 0,1	0,10 ± 0,0	3,33 ± 0,0	0,14 ± 0,0	0,031

Table 4 *- Energy dispersive X-ray surface analysis of the obtained copper doped titanium dioxide layer under varying conditions. Calculated calcium over phosphorous ratio for the measured atomic percentages.*

Condition	Ti [at %]	O [at %]	Ca [at %]	P [at %]	Cu [at %]	Ca/P [-]
0.1 g/L Cu	26,98 ± 0,2	68,32 ± 0,2	0,53 ± 0,0	3,83 ± 0,0	0,35 ± 0,1	0,138
0.3 g/L Cu	28,72 ± 0,2	67,08 ± 0,2	0,25 ± 0,0	3,63 ± 0,1	0,33 ± 0,1	0,069
0.5 g/L Cu	28,79 ± 0,2	66,66 ± 0,2	0,30 ± 0,0	3,66 ± 0,1	0,61 ± 0,1	0,082
0.8 g/L Cu	27,21 ± 0,1	67,57 ± 0,1	0,51 ± 0,0	4,23 ± 0,0	0,50 ± 0,1	0,121

Figure 22 and Figure 23 both illustrate the EDX analysis over the entire layer depth until close to the bulk where presence of both calcium and phosphorous is confirmed. A non-homogeneous distribution of the particles can be hypothesised. Figure 22 clearly indicates the presence of the antibacterial silver while the presence of copper in Figure 23 is less indicative. The measure is namely greatly influenced by noise since the sample holder itself consists of copper possibly falsely increasing the detected atomic percentage.

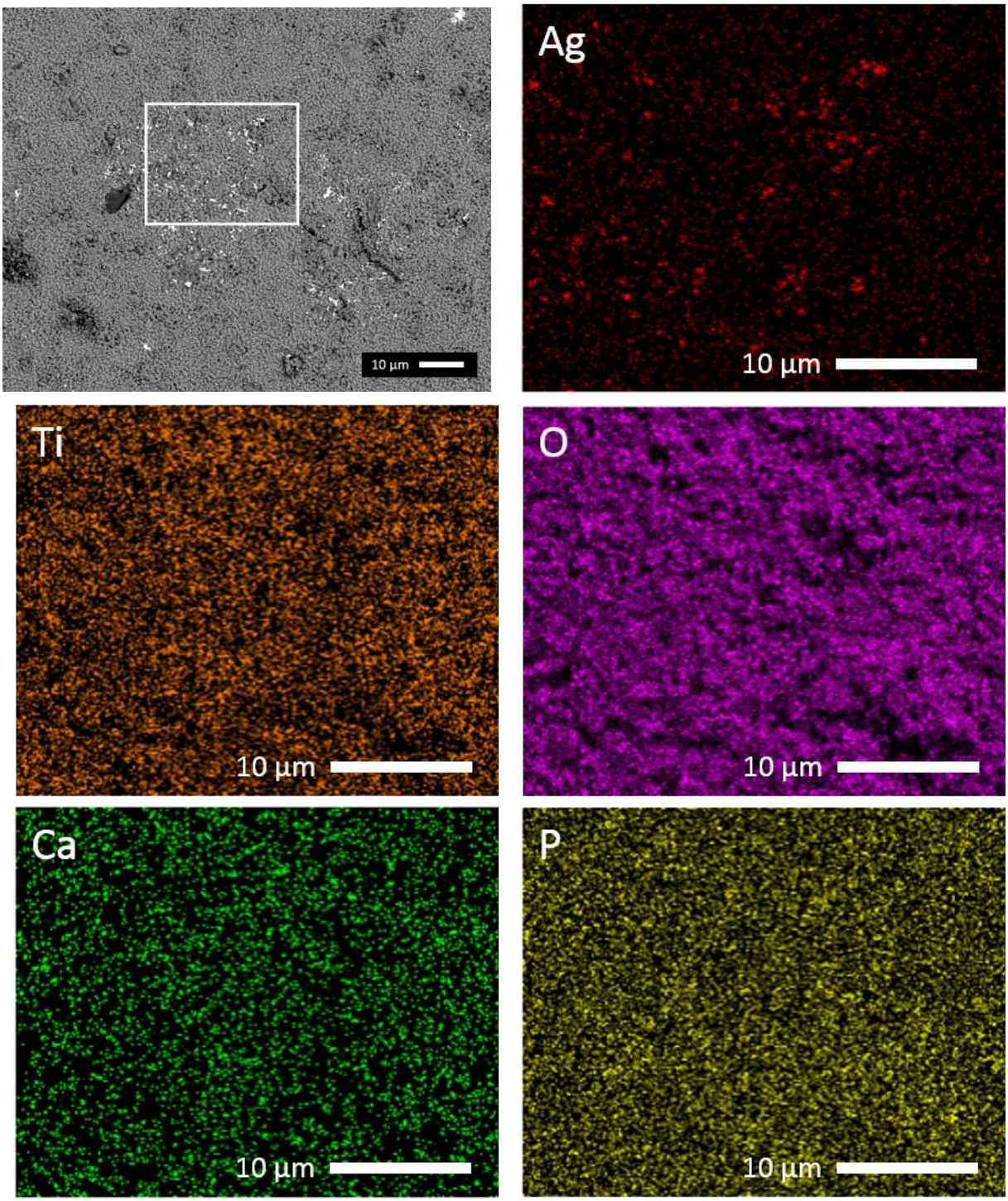

Figure 22 *- Surface EDX analysis of the silver doped titanium dioxide layer under 0,8 g/L condition at a magnification of 1000x.*

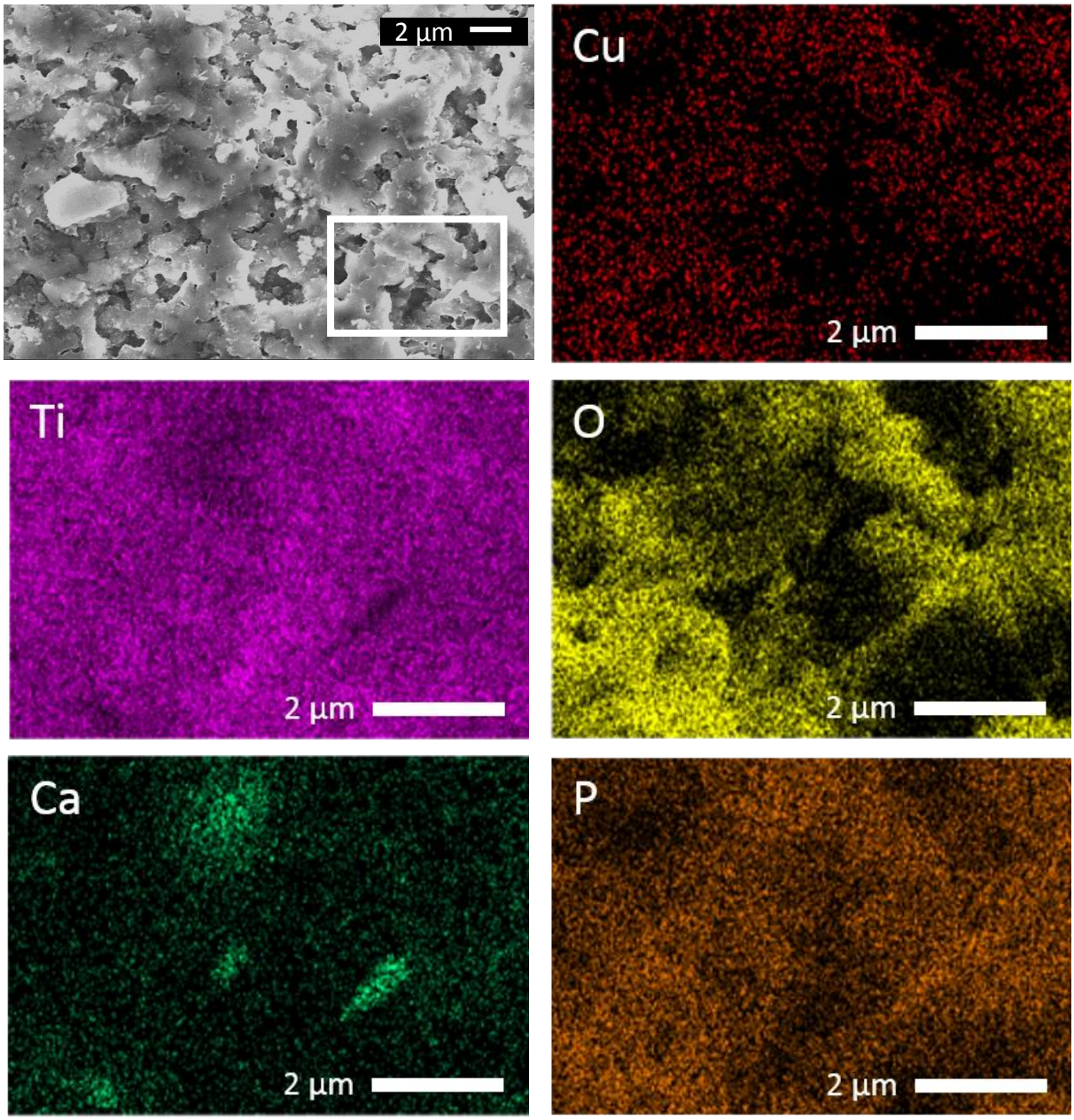

Figure 23 *- Surface EDX analysis of the copper doped titanium dioxide layer under 0,8 g/L condition at a magnification of 5000x.*

Cross sectional analysis was performed to study the variance of the titanium dioxide layer over its depth with the main focus on the fluctuation in the elemental distributions, to validate the hypothesis stated above. First of all, cross sectional EDX did confirm the presence of all elements detected via surface EDX. However, The distribution of these elements appears not homogeneous over the depth of the layer as illustrated in Figure 25. The upper layer of the titanium bulk sample transforms to titanium dioxide by plasma electrolyte oxidation, which is called the first sublayer. This layer which is closer to the bulk is enriched in phosphorous

elements. The formed porous titanium dioxide layer is also deposited as a coating on the titanium sample, this rather elevated second sublayer at the surface is enriched in calcium atoms in the oxygen rich areas. These findings confirm the previously discussed XPS and EDX data already indicating the rather elevated calcium settlement in the layer compared to phosphorous. As explained before, PEO is a step-wise process with continuous alternating oxide formation and breakdown. The porous outer layer of the coating is repeatedly created and destroyed by micro arcs and its growth originates primarily from electrolyte material rather than from the bulk elements. As this electrolyte is characterised by a greater calcium concentration compared to phosphorous, an increased calcium concentration is expected in the outer layer. Titanium on the other hand is only present as bulk material and is therefore expected to be the main component of the rather compact surface layer.

It can thus be stated that both calcium and phosphorous are incorporated in the oxygen rich sections of the antibacterial layer, but that the separation of the elements hinders the direct formation of hydroxyapatite. Secondly the lack of present calcium to obtain the preferred ratio of 1,67 is confirmed in these EDX distribution images. Further optimization of the plasma oxidation parameters and electrolyte concentration is needed to attain the desired osteogenic promoting antibacterial titanium dioxide layer.

The presence of the antibacterial silver atoms over the entire titanium dioxide layer depth is confirmed in Figure 25. A more or less homogeneous distribution of these particles is seen, and no cluster formation is detected after this stage of the process. The latter promotes the use of antibacterial silver salts over their pure nanoparticle variant. The cross sectional EDX analysis of the copper doped titanium dioxide layer given in Figure 27 was less indicative regarding the copper distribution as the measurement was influenced by a lot of noise.

The porous morphology of the coating can also be observed from the cross sectional SEM images shown in Figure 24 and Figure 26 . Overall the titanium dioxide layer appears to be advantageous with varying morphology and depth. On average the layer thickness can be stated around one to two micrometer.

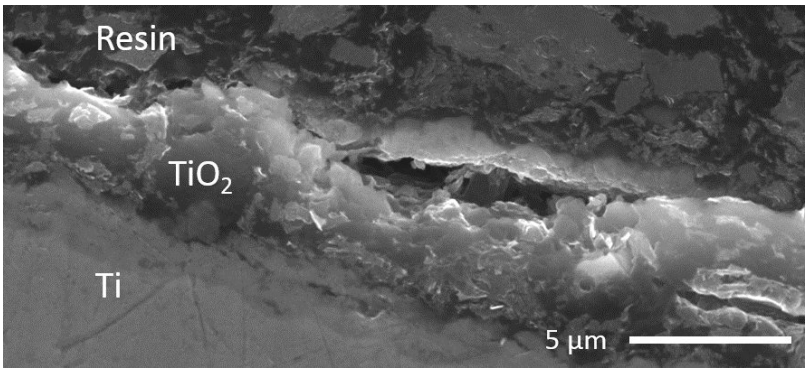

Figure 24 *– Cross sectional analysis illustrating the porosity and surface morphology of the 0,8 g/L silver doped titanium dioxide layer at a magnification of 5000x.*

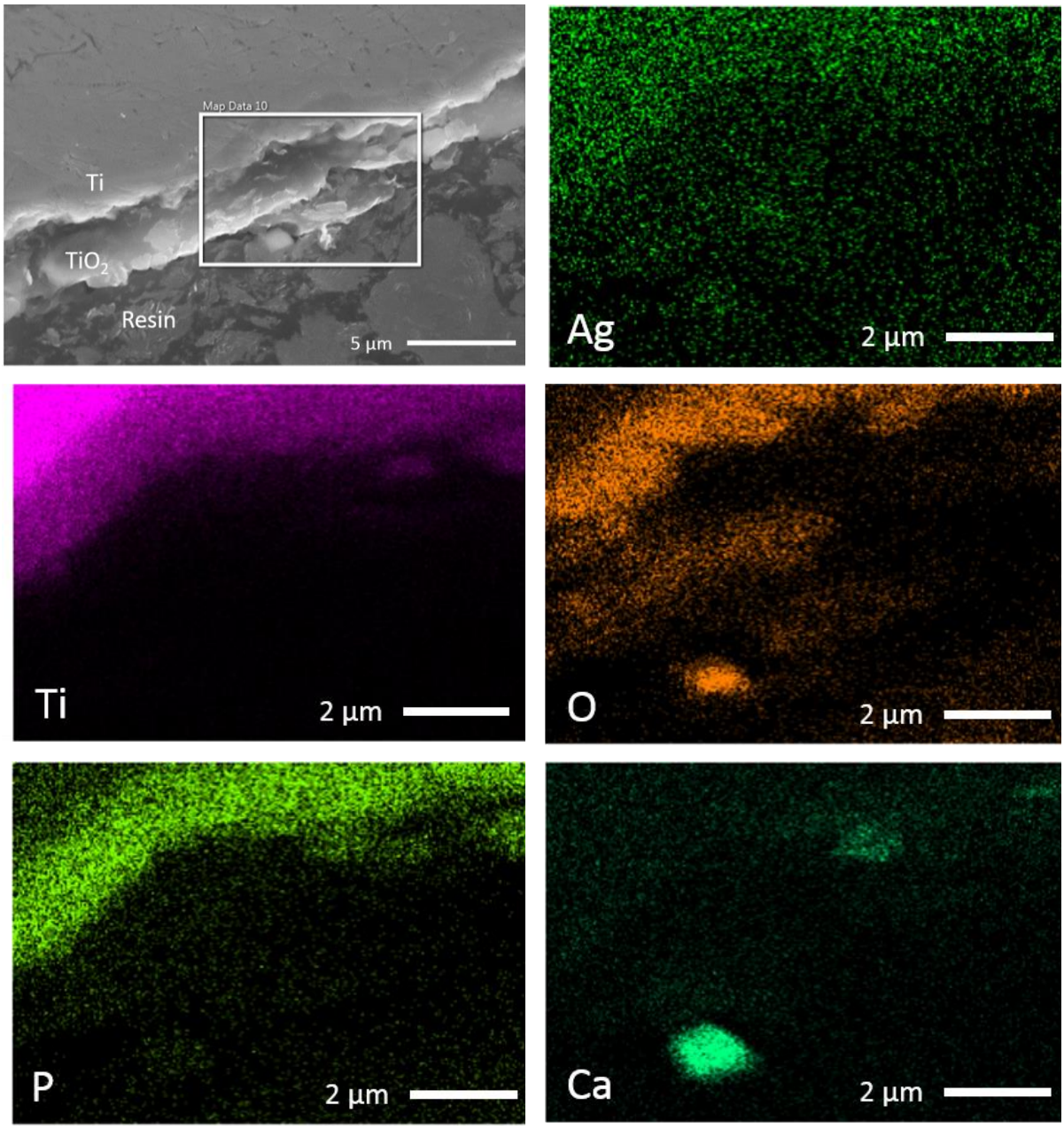

Figure 25 *- Cross sectional EDX analysis indication the variation in element distribution over the depth of the 0,8 g/L silver doped titanium dioxide layer at a magnification of 5000x.*

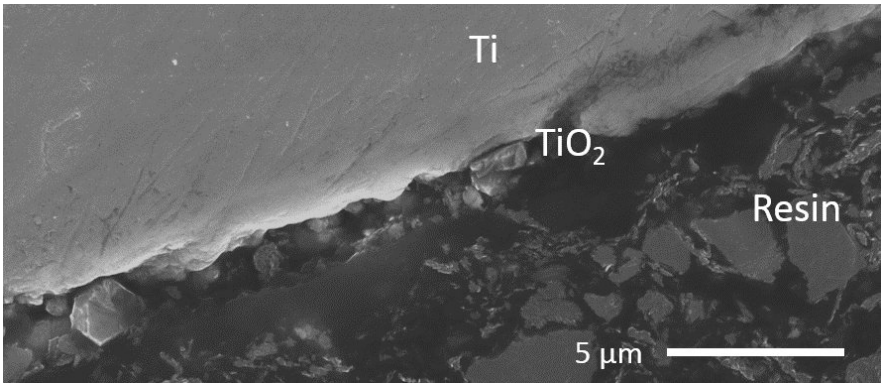

Figure 26 *- Cross sectional analysis illustrating the porosity and surface morphology of the 0,8 g/L copper doped titanium dioxide layer at a magnification of 5000x.*

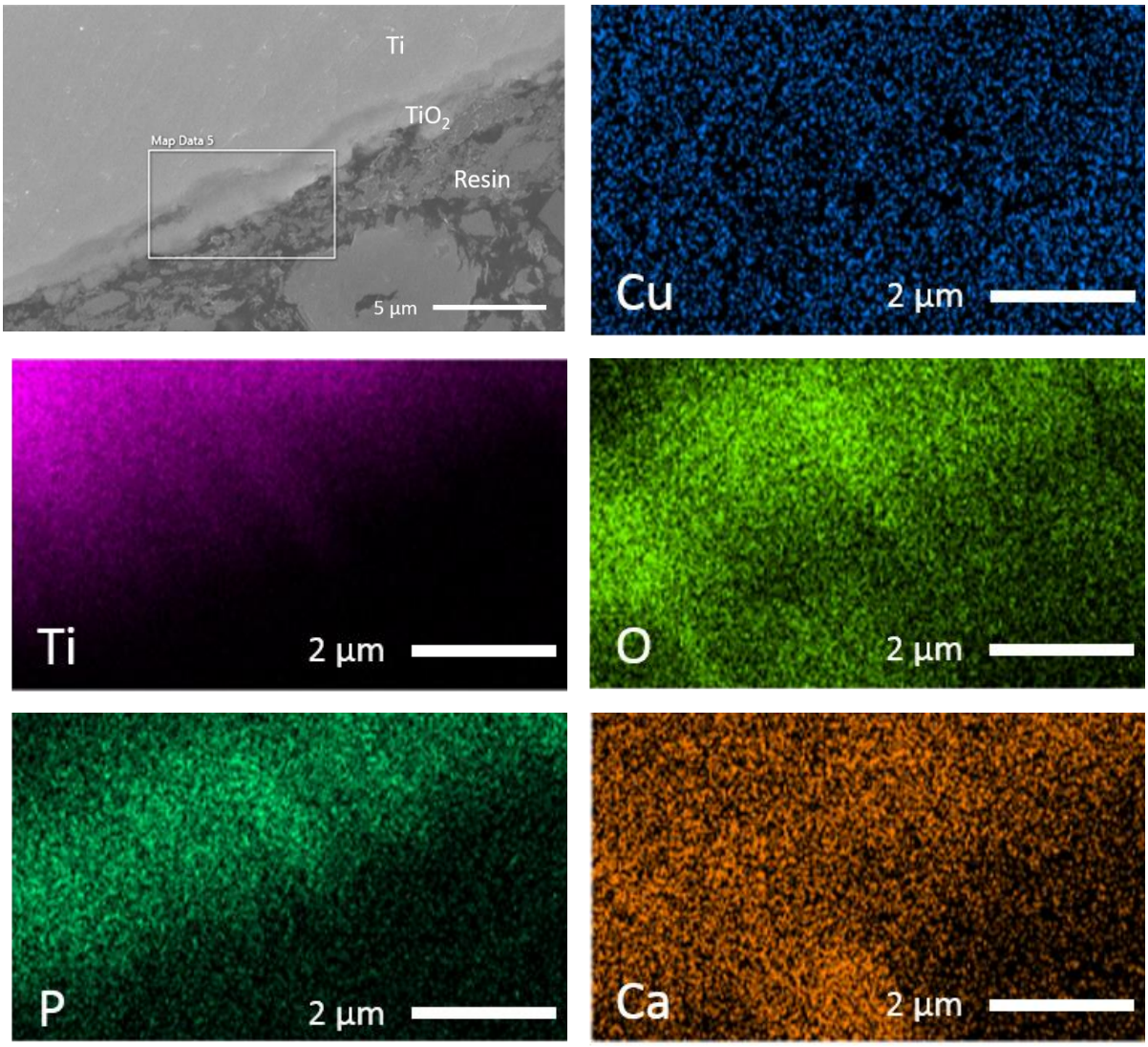

Figure 27 *- Cross sectional EDX analysis indication the variation in element distribution over the depth of the 0,8 g/L copper doped titanium dioxide layer at a magnification of 5000x.*

13 AFM

Atomic force microscopy was used to determine the roughness of the titanium dioxide layer. The surface roughness is defined as the average vertical deviation from nominal surface over a certain length. AFM is limited by its resolution to a certain extent. In non-contact mode the cantilever oscillates at an amplitude of only a few nanometres so surface roughness above ten nanometers can't be detected. In tapping mode, the analysis depth is somewhat increased to a few hundred nanometres due to the greater oscillation amplitude. The range of both operating modes doesn't cover the full depth of the titanium dioxide layer to get an accurate surface roughness [58]. Deviations can be expected if analysis is performed on top or inside of a pore, so a great influence of the layer porosity and its homogeneity is expected. Therefore, several roughness measurements should be averaged to attain a representative result.

In Figure 28 the AFM image indicates the roughness of the silver doped oxide layer, averaging the computed data results in an overall roughness of 112,7 nm. The same was done for the copper doped layer of which the results are given in Figure 29 and an average surface roughness of 102,4 nm was determined. First of all, it can be concluded that the metallic salt added to the electrolyte doesn't influence the roughness. Furthermore, the expected surface roughness in the order of micrometer couldn't be detected via the scanning force microscopy technique due to its restricted resolution.

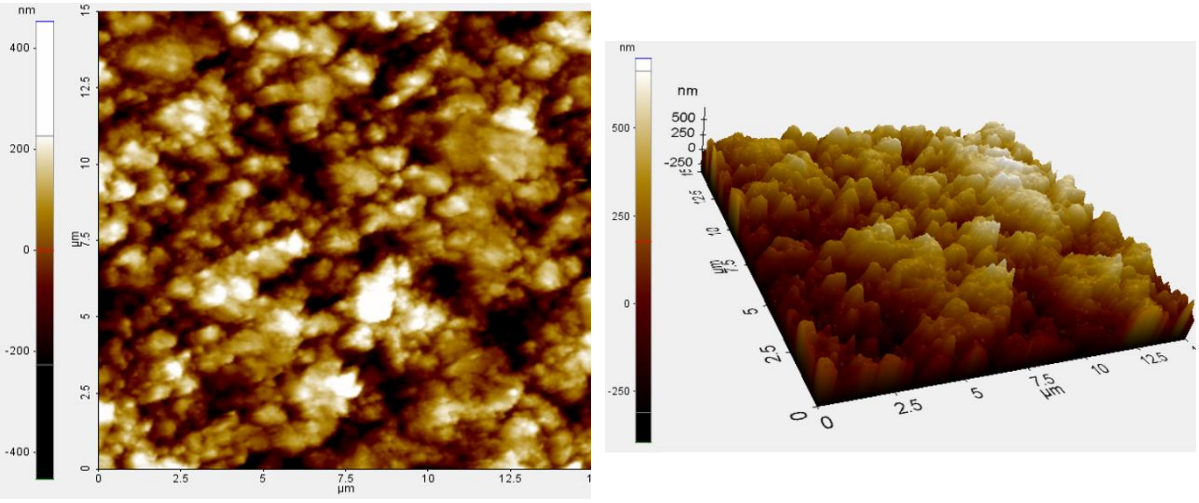

Figure 28 *- AFM images illustrating the nanometer scale roughness of the silver doped titanium dioxide layer.*

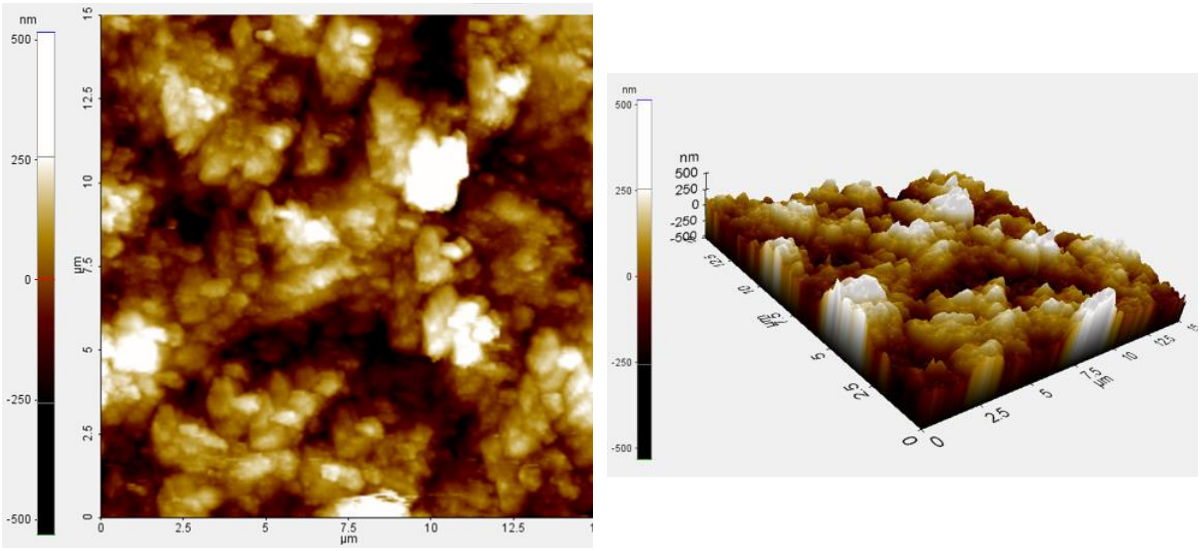

Figure 29 *- AFM images illustrating the nanometer scale roughness of the copper doped titanium dioxide layer.*

14 ICP-MS

When a silver doped TiO_2 coated sample is in contact with aqueous medium, silver ions will be generated. The antibacterial efficiency of the coating is related to its silver ion release profile. Therefore, it is important to quantify the silver ion release rate using ICP-MS. A higher initial concentration in the titanium dioxide layer results in a greater particle release as can be seen in Figure 30. Overall a quick burst release is seen within the first few hours of immersion after which the release rate decreases. It can be expected that a saturation will be reached in which antibacterial particles are no longer released from the titanium dioxide layer. This saturation is proposed earlier for smaller silver concentrations.

From the examined time period of 17 days no prediction can yet be made about the point of saturation. The applications of antibacterial titanium implants however have a time range of a few weeks to months and even up until several years. Ideally during this whole period, the antibacterial properties are preserved without being too large such that no cytotoxicity is induced. Therefore, a prolonged ICP-MS analysis is needed to determine the complete time range of silver release.

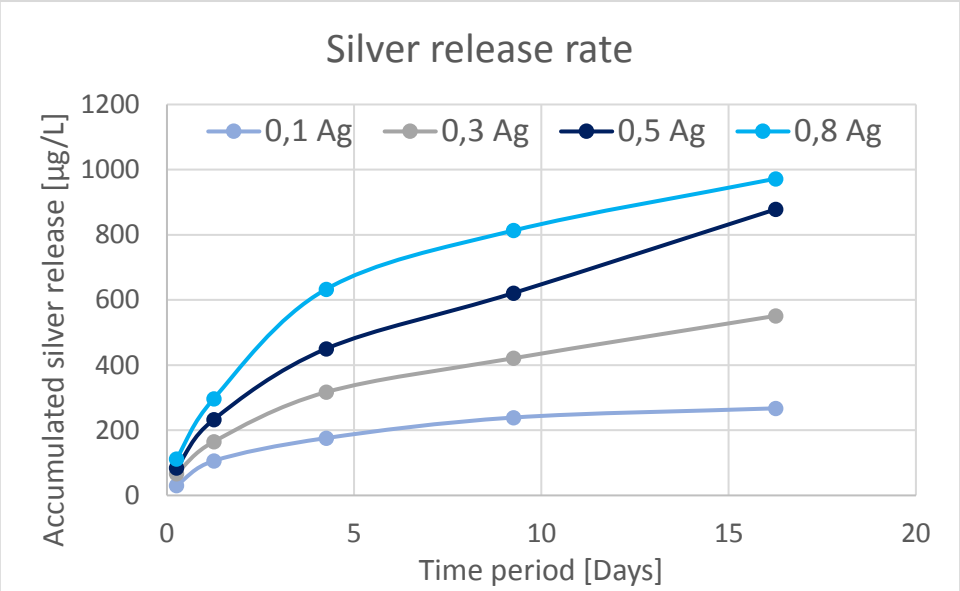

Figure 30 *- ICP-MS analysis illustrating the silver release kinetics.*

15 Antibacterial test

The antibacterial activity of the titanium dioxide coating is examined by in-vitro assay and results are illustrated in Figure 31 and Figure 32. For the untreated titanium sample, no bacterial reduction was observed for both microorganisms. The presence of silver and copper particles on the other hand induced a substantial decrease in bacterial counts with an increasing bacterial reduction at higher silver or copper concentrations. The release of silver or copper ions and/or the release of free radicals in the liquid medium caused this great reduction in number of bacteria.

Overall a slight superiority of silver is seen over copper regarding its antibacterial activity. This difference is however restricted to a minimum imposing both elements as candidates of metallic salts to be incorporated in the titanium dioxide layer. Both silver and copper illustrate more or less equal activity against both E. coli and S. aureus bacteria indicating that these antibacterial compounds can sufficiently oppose implant related infections. Bacterial growth is not completely precluded, but an inhibition of over 99% which is obtained even for the smallest concentration, which is sufficient to speak of complete antibacterial activity.

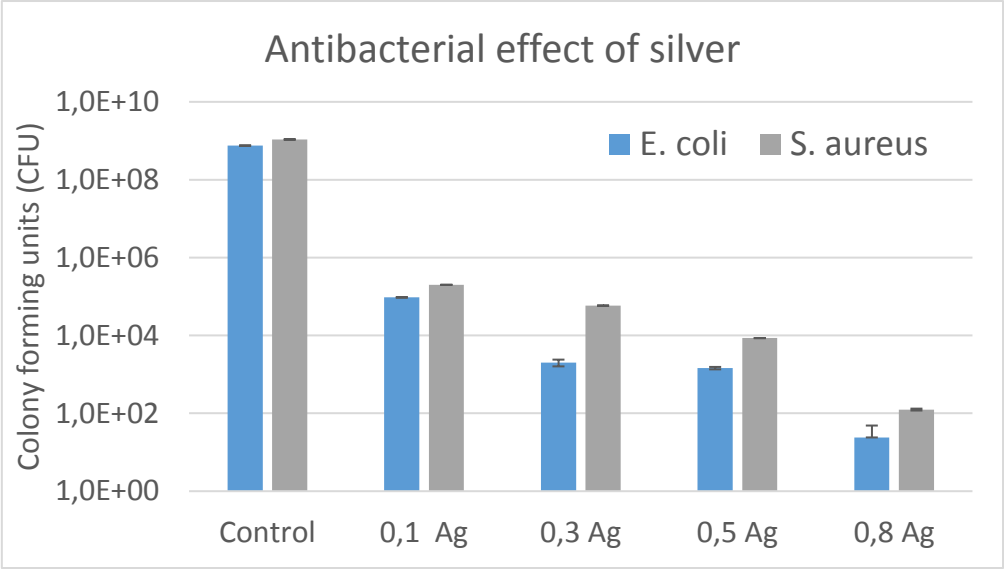

Figure 31 *- Reduction in the number of E. coli and S. aureus bacteria by the silver incorporated in the titanium dioxide layer.*

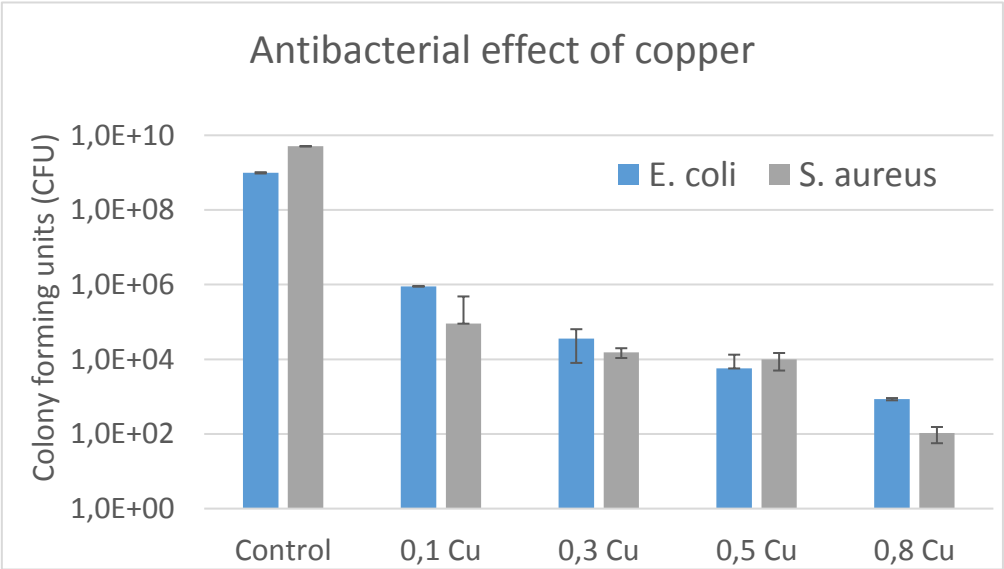

Figure 32 *- Reduction in the number of E. coli and S. aureus bacteria by the copper incorporated in the titanium dioxide layer.*

16 Cytotoxicity test

Besides its antibacterial properties, the titanium dioxide layer should also possess cytocompatibility. The biocompatible properties of any surface are influenced by its surface properties such as surface morphology, surface wettability and its chemical constituents which can promote cell growth and proliferation. From the SEM and XPS analysis it was observed that the coating has a porous morphology which can help to anchorage the cells and

the presence of calcium and phosphorous is expected to promote cell growth and proliferation. Water contact angle analysis showed that the surface changed from hydrophobic in the case of untreated titanium (70°) to more hydrophilic TiO_2 ($\pm$ 20°) which enables spreadabilty of the cells. In order to evaluate the cytocompatibility of the surface, MTT, live/dead staining and SEM analysis were performed of which the results are illustrated below.

16.1 SEM and fluorescence visualisation

Figure 33 illustrates the cell morphology and their viability one day after seeding through fluorescence and SEM microscopy. The SEM image in the top row of Figure 33 indicates that in case of untreated titanium surface cells exhibited a round morphology. This indicates the low affinity of the cells for this surface. The coated samples on the other hand exhibited a more flattened and elongated spindle cell morphology indicating great initial adhesion. From live-dead fluoroscopy it can be seen that 1 day after cell seeding, the titanium dioxide layer does not really influence the cell viability and in fact all conditions impose more or less the same viable cell characteristics. The bottom row of Figure 33 illustrates the reduced cell viability in case of the coating with the highest silver concentration. It can thus be hypothesised that a too large silver concentration can cause toxicity to the cells and inhibit cell adhesion.

In both Figure 33 and Figure 34 a deviation in the SEM images is seen for the silver doped layer under 0,3 g/L Ag electrolyte condition. This may be due to an experimental error which occurred during the plating procedure or the fixation afterwards.

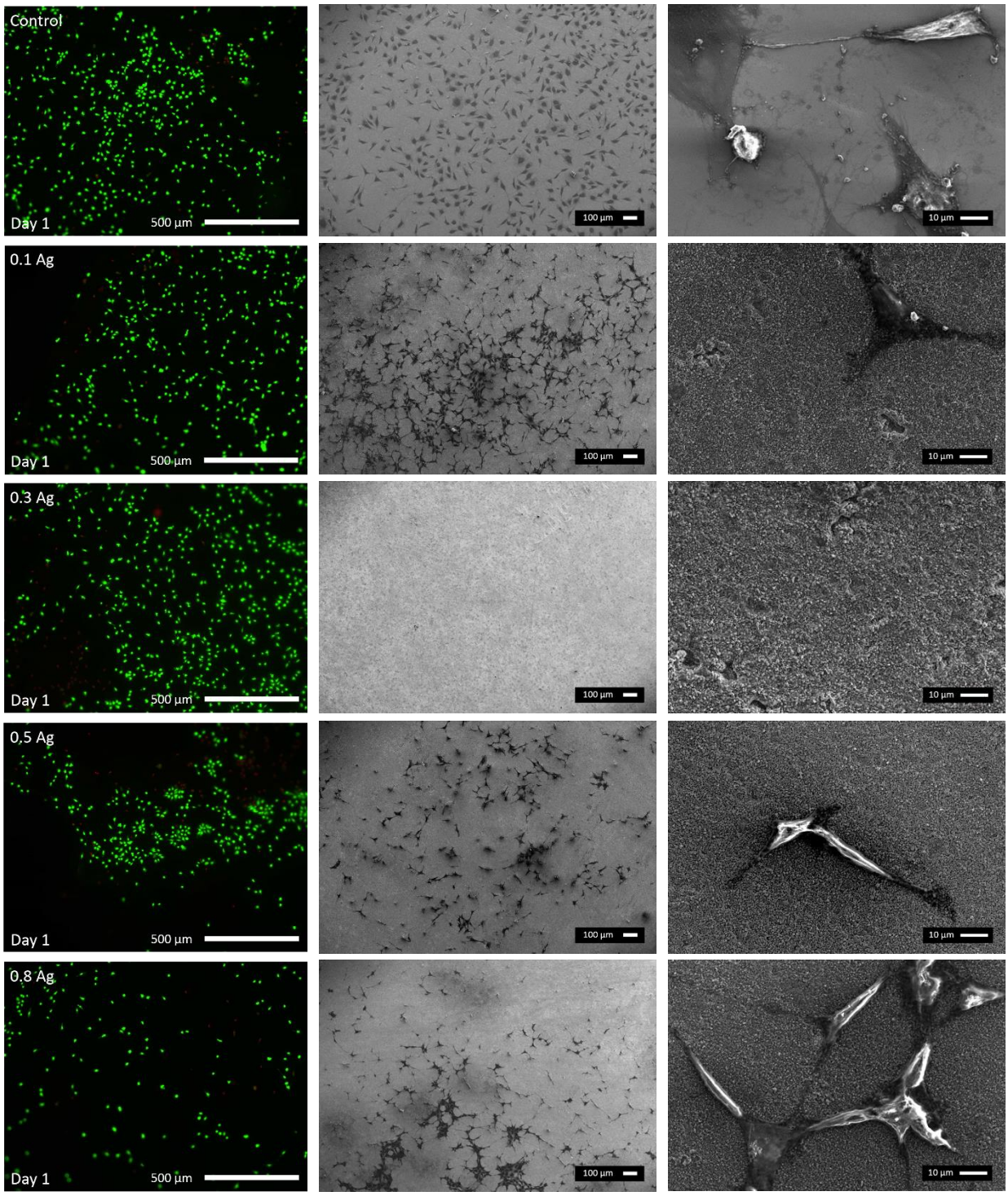

Figure 33 *– Fluorescence and SEM images taken one day after seeding the cells on the varying surfaces. Left: Fluorescence indication cell viability. Magnification 4x. Middle: SEM illustrating cell adherence. Magnification 50x. Right: SEM illustrating cell morphology. Magnification 1000x. Top: Untreated titanium control sample.*

Fluorescence and SEM were also acquired seven days after seeding to examine cell proliferation. Overall an increased cell density is seen both in fluorescence and SEM images due to the seven-day growth and division period. For the untreated titanium sample, no

change in the round cell morphology can be observed in Figure 34. The spindle morphology of the cells is exhibited for all silver doped samples indicating that the surface not only favours good initial adherence but also a favours cell-surface interaction. The latter is also seen in the restricted amount of cluster formation seen in SEM, caused by cell-cell interactions. Fluorescent density indicates the cell preference for the silver doped titanium dioxide layer over untreated titanium resulting in an increased viable cell density on the coated samples. When comparing the different silver concentrations, no clear difference is seen in fluorescence indicating no direct relation between too large silver concentrations and toxicity.

It has to be mentioned that the staining used on day seven was not of ideal quality resulting in a lot of fluorescence background influencing the fluorescent images and the cytotoxicity analysis. In order to attain more accurate cell toxicity information the test has to be re-done.

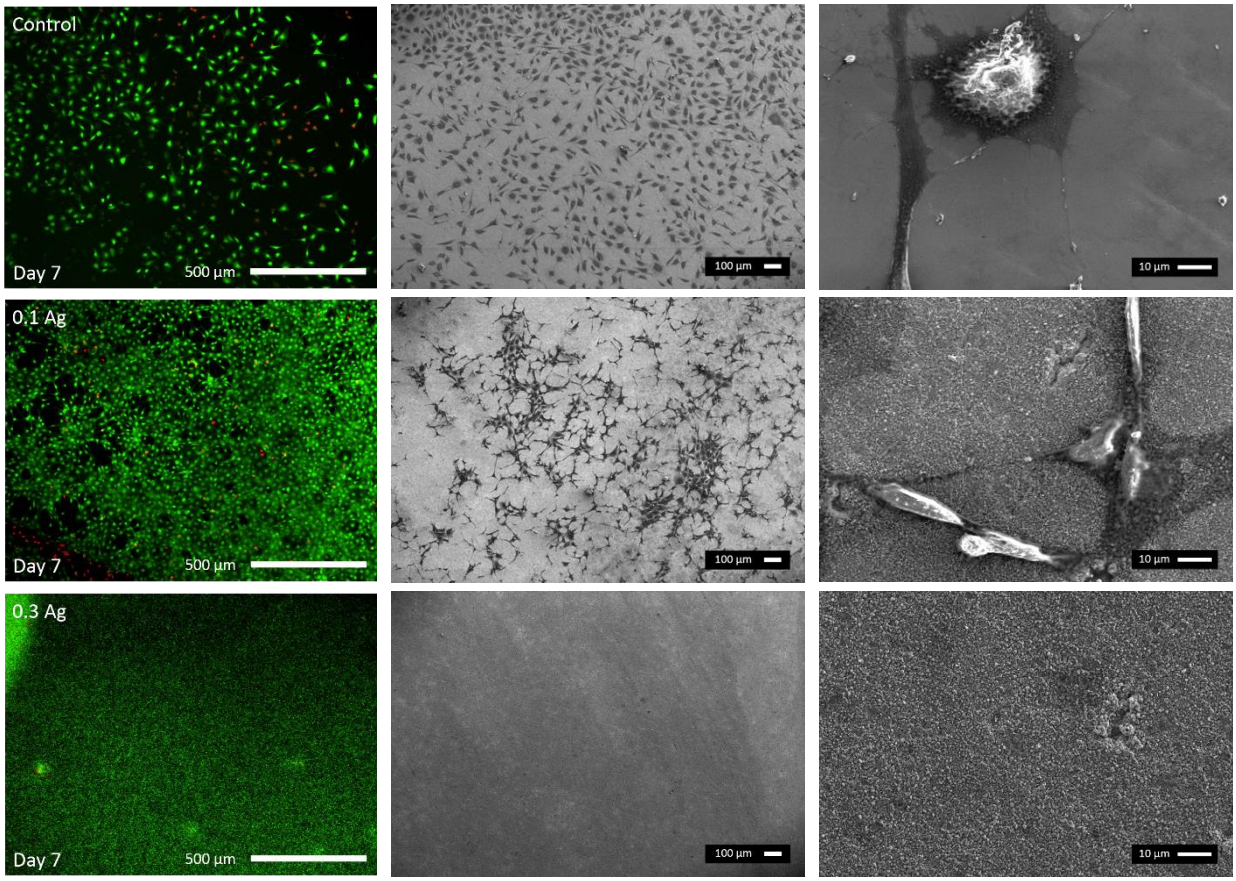

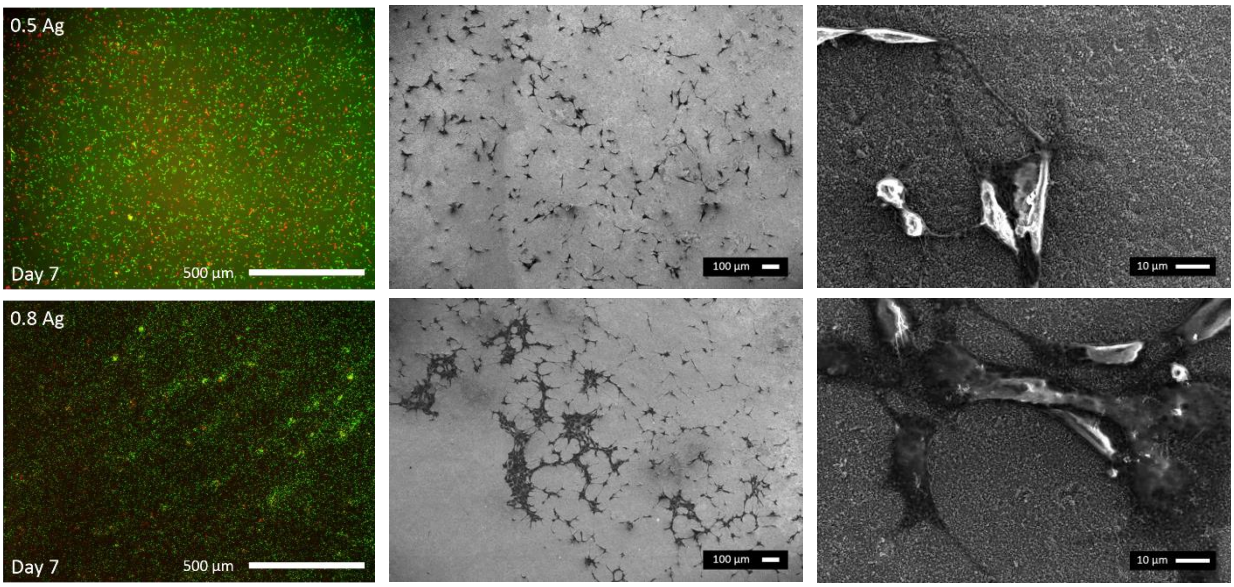

Figure 34 *- Fluorescence and SEM images taken seven days after seeding the cells on the varying surfaces. Left: Fluorescence indication cell viability. Magnification 4x. Middle: SEM illustrating cell adherence. Magnification 50x. Right: SEM illustrating cell morphology. Magnification 1000x. Top: Untreated titanium control sample.*

16.2 MTT analysis

SEM and fluorescence only provide qualitative insights in cytotoxicity, MTT analysis was used to quantify the number of viable cells. From figure 34 it can be observed that all silver doped titanium dioxide coated surfaces exhibited increased cell viability compared to the untreated titanium. The samples with less silver content (0,1; 0,3 and 0,5 g/l) exhibited almost 90% cell viability, therefore it can be stated that all layered samples are considered to be biocompatible according to the ISO 10993-5:2009 standard, stating that a medical device is biocompatible up until a decreased viability of 30% [59]. MTT results indicate that overall the titanium dioxide layered samples impose a larger MC3T3 cell viability due to the incorporated calcium and phosphate atoms mimicking hydroxyapatite. It appears that not only these osteogenic promoting elements, but also the antibacterial particles influence the cell viability. The layered samples obtained from a 0,3 g/L or 0,5 g/L silver electrolyte concentration are most favourable with a biocompatibility exceeding the positive control TCPS. Overall an increase in cell viability is seen at day seven caused by cell proliferation over time.

While a certain amount of antibacterial particles appear to up-regulate certain cell proteins increasing their proliferation enhancing cell viability, a too large occupancy of these particles downregulates the cell viability. The latter causes an uncontrolled interaction of the silver particles with various macromolecules causing damage and increasing oxidative stresses. This on its turn disrupts cellular processes and triggers apoptosis [60]. This affirms the presumption stated before that the 0,8 g/L Ag condition induces toxicity due to its too large silver concentration in the titanium dioxide layer.

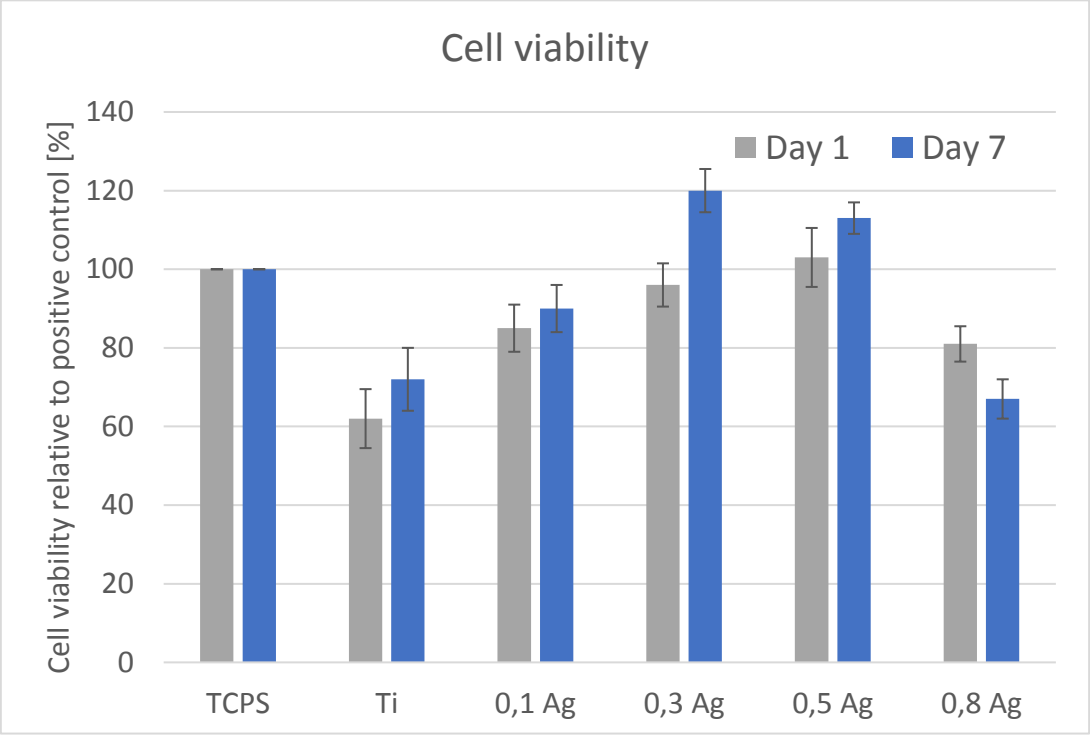

Figure 35 *- MTT analysis indicating cell viability relative to TCPS of the untreated Ti and the TiO_2 layer under varying antibacterial silver conditions.*

17 Scratch test

Pin on disc tribology testing allows to determine the dynamic coefficient of friction of the samples. This test was performed to mimic a first potential application of antibacterial coated titanium such as bone screws. As screwing in a bone or a plate is needed, the coating should be able to withstand this friction force and have a high enough wear resistance such that no abris is released in the body and the titanium dioxide layer preserves its antibacterial properties. A scratch test only mimics this handling to a certain extent. Ideally friction,

hardness and compression should be verified as well in order to assure layer preservation in bone screw applications.

The coefficient of friction describes the ratio of the friction force applied between two surfaces and the normal force pressing them together. Generally rougher surfaces tend to have a greater coefficient of friction than smooth once. The pin on disk tribology test confirmed this also applies for the examined titanium samples as can be seen in Figure 36. The smooth polished untreated titanium samples are characterised by a smaller coefficient of friction than the rougher samples containing a porous titanium dioxide layer at the surface. Ideally the coefficient of friction is not proportional to the applied normal force. A certain trend however is seen in the tribology test data. Since different test samples were used for different applied loads, the differences can be explained independently of the normal force and purely by the performed sample preparation and PEO conditions.

It has to be noted that a friction coefficient is not a direct material property, but rather expresses the relation between two materials. The indenter used in the tribology set-up is made of steel which might differ from the material the titanium bone screws will be in contact with under in vivo conditions. This test therefore only serves as first estimate of the mechanical properties of the porous titanium dioxide layer.

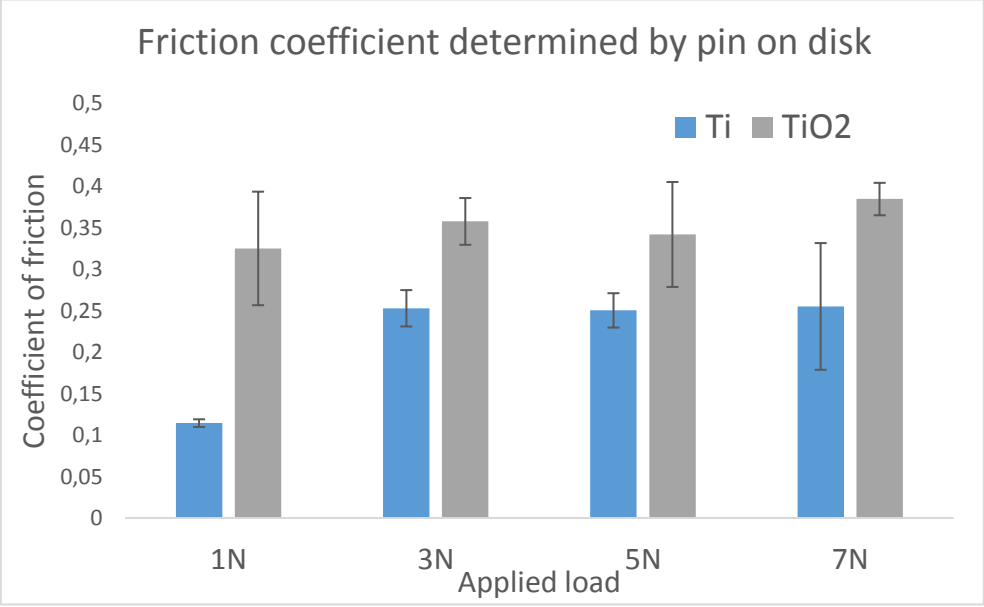

Figure 36 *- Comparison of the coefficient of friction of bulk titanium and a 0,1 g/L silver doped titanium dioxide layer under varying loads.*

Atomic force microscopy was used to analyse the depth of the scratch. As expected, a greater applied load results in a greater depth of scratch. In Figure 37 the scratch depth analysis indicates that generally the pin indented the sample a few hundred nanometers which doesn't exceed the depth of the titanium dioxide layer. Despite the porous morphology of the latter a smaller depth of the scratch is obtained compared to untreated titanium. This can be explained by the hardness of these surface materials. Titanium is characterised by a Vickers hardness between 830 MP and 3420 MP [61] while titanium dioxide can reach a Vickers hardness up to 38 GP [62]. However, this hypothesis was not tested nor confirmed on the coated samples in this research.

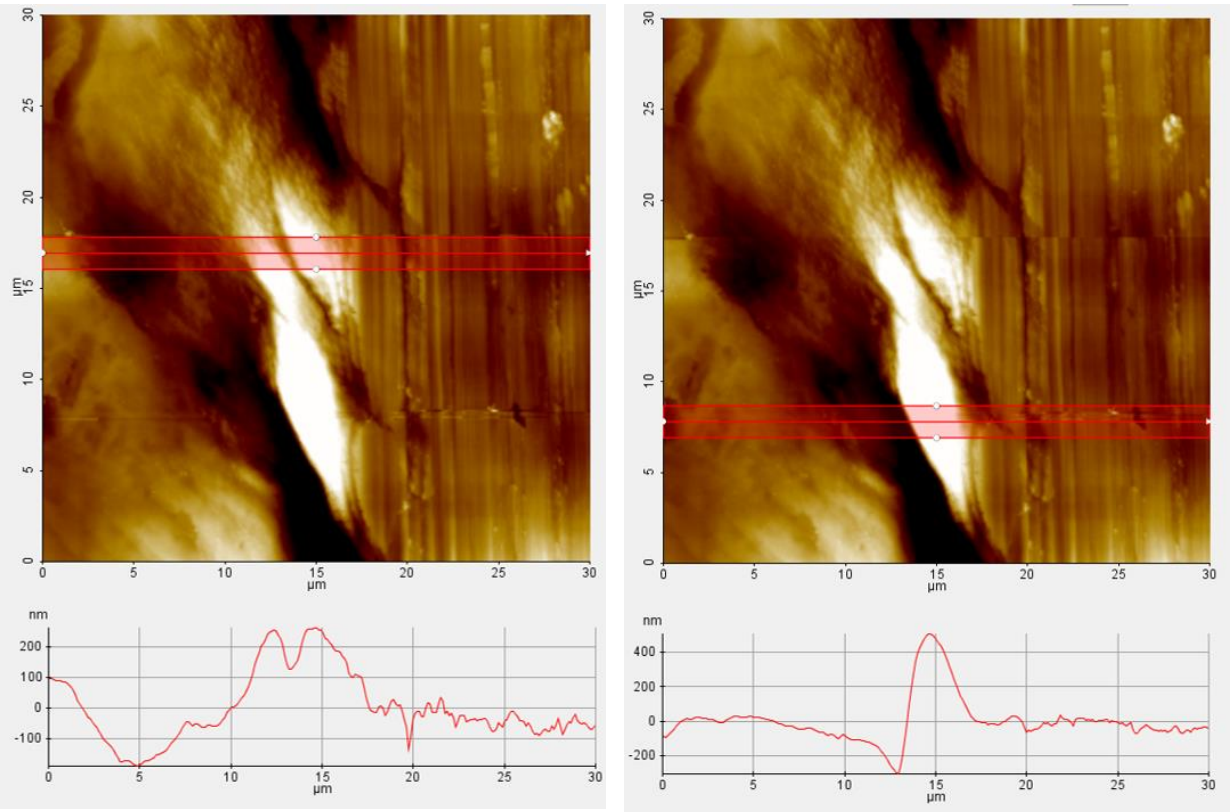

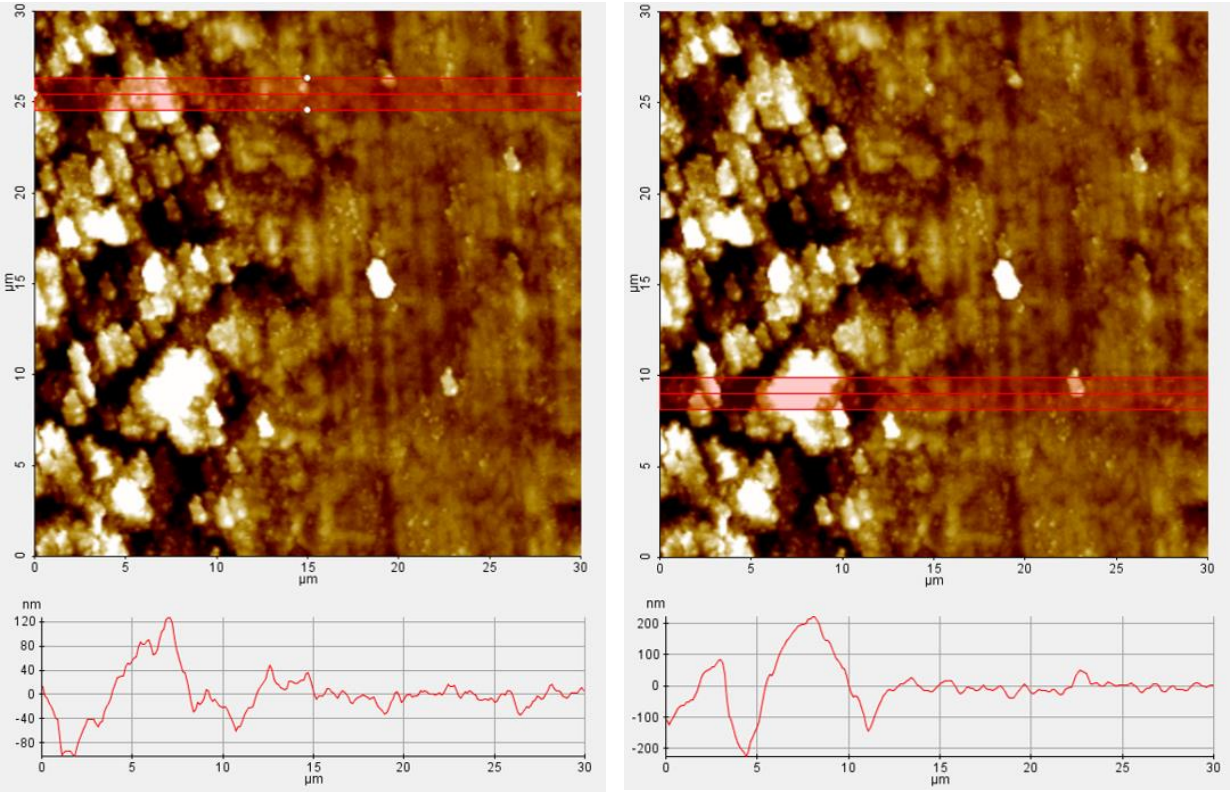

Figure 37 *- AFM analysis of the scratch morphology and depth for an applied load of 5N. Top: Bulk titanium. Bottom: 0,1 g/L silver doped TiO_2 layer.*

Conclusion

The objective of the thesis was to develop both an antibacterial and biocompatible porous titanium dioxide layer through plasma electrolyte oxidation. Through optimization of the electrolyte concentration and process parameters this goal was achieved with an electrolyte composition of 2 g/L NaH_2PO_4-$2H_2O$, 5 g/L $Ca(OOCCH_3)_2$-H_2O and 0,1; 0,3; 0,5 or 0,8 g/L $AgOOCCH_3$ or $Cu(OOCCH_3)_2$.

XPS analysis confirmed the presence of calcium and phosphorous to a sufficient extent to promote osteogenic properties and the presence of silver and copper both possessing antibacterial properties. Their incorporation was confirmed by EDX surface and cross-sectional analysis indicating the particle distribution and inhomogeneity over width and depth of the layer. Phosphorous can be found close to the bulk while the surface is enriched in calcium both in oxygen abundant areas. SEM and AFM analysis illustrated the favoured porous surface morphology with a surface roughness around hundred nanometres.

Besides the chemical characteristics also the biological properties of the coating were studied. ICP-MS evinced the release of the antibacterial particles from the porous layer. This release is preserved during the first few days with decreasing kinetics over time and an expected saturation after a few weeks. The functionality of this release was proven by the antibacterial tests performed on E. coli and S. aureus bacteria where bacterial growth was reduced by 99% even for the smallest concentration and the bacterial reduction was increased with increasing Ag/Cu concentrations. A limit to this increase was imposed by the cell viability analysed with MTT which indicated reduced cell viability for the 0,8 g/L sample caused by their toxic side effects. Biocompatibility was proven for the 0,1; 0,3 and 0,5 g/L silver doped conditions with the latter two even exceeding the cell viability of the positive control. Finally, SEM analysis revealed the favoured cell-surface interaction resulting in a more spread out spindle cell morphology on the treated samples compared to the untreated titanium control.

At last the mechanical properties of the porous titanium dioxide layer were tested via a pin-on-disk scratch test. The surface roughness induced a greater friction coefficient between the steel indenter and the treated surface than the untreated titanium. Secondly the hardness of the titanium dioxide resulted in a restricted scratch depth compared to untreated titanium. Both properties favour the use of the coated titanium in orthopaedic applications such as bone screws.

Overall it can be concluded that the chemical and mechanical properties of the porous layer are advantageous for its use in medical implant applications. The cytocompatibility properties indicated an upper limit for the incorporated concentration of antibacterial particles. ICP-MS on the other hand implies a lower limit to this concentration to assure prolonged release over time. An optimal trade-off between them should be found.

Future work

First of all, more analysis has to be performed on the copper doped titanium dioxide layer in order to make a complete comparison between the two antibacterial coatings. Due to time limitations the ICP-MS and cytotoxicity analysis were not performed therefore no information is known about the release mechanics of the copper particles and the interaction between the copper doper TiO_2 layer and osteogenic MS3T3 cells. Analysis is needed to determine the lower and upper concentration limit of copper.

Besides the revision of certain tests, extra assessments are needed as well, especially to test the mechanical properties of the layer. For example, the layer hardness and wear resistance under in vivo conditions should be tested. Besides these mechanical tests, a prolonged ICP-MS analysis has to be performed to determine the point of saturation and compare this to the antibacterial need of the medical implant.

Despite the limited calcium to phosphorous ratio a great cell-surface interaction promoting cell growth is already seen. Cell viability could possibly be even further increased through the addition of extra calcium into the layer. Examination of the electrolyte and device parameters is needed to determine the maximal reachable Ca/P ratio. Cell viability testing should thereafter be performed to evaluate the influence of variations in the calcium concentration.

Finally, the PEO process parameters should be adapted and optimised to allow layer deposition on screw shaped samples instead of flat plates. This allows analysis of shape induced layer inhomogeneities and imperfections. Secondly, more accurate mechanical testing on these samples is needed since no existing test can mimic the bone screw as good as the actual handling.

References

[1] I. De Graeve, “Biomaterials - Partim Biometals,” 2018.

[2] L. Visai *et al.*, “Titanium oxide antibacterial surfaces in biomedical devices,” *Int. J. Artif. Organs*, vol. 34, no. 9, pp. 929–946, 2011.

[3] L. Zhao, P. K. Chu, Y. Zhang, and Z. Wu, “Antibacterial coatings on titanium implants,” *J. Biomed. Mater. Res. - Part B Appl. Biomater.*, vol. 91, no. 1, pp. 470–480, 2009.

[4] Y. Wang, H. Yu, C. Chen, and Z. Zhao, “Review of the biocompatibility of micro-arc oxidation coated titanium alloys,” *Mater. Des.*, vol. 85, pp. 640–652, 2015.

[5] H. Cao and X. Liu, “Activating titanium oxide coatings for orthopedic implants,” *Surf. Coatings Technol.*, vol. 233, pp. 57–64, 2013.

[6] U.S. Food and Drug Administration, “Implants and Prosthetics,” 2018. [Online]. Available: https://www.fda.gov/medicaldevices/productsandmedicalprocedures/implantsandprosthetics/. [Accessed: 15-Dec-2018].

[7] Frederick H. Silver, *Biomaterials, Medical Devices and Tissue Engineering: An Integrated Approach*. Dordrecht: Springer Science+Business Media.

[8] K. Prasad *et al.*, “Metallic Biomaterials : Current Challenges and Opportunities.”

[9] “kidshealth.” [Online]. Available: https://kidshealth.org/EN/images/illustrations/exFixPinCare_a_enIL.png. [Accessed: 29-Apr-2019].

[10] R. E. Buckley and C. Colton, “AO Surgery Reference.” [Online]. Available: https://www2.aofoundation.org/wps/portal/surgery?showPage=redfix&bone=Tibia&segment=Shaft&classification=42-Special considerations&treatment=&method=Special considerations&implantstype=Infection&approach=&redfix_url=1341319024234&Lan

guage=en. [Accessed: 10-May-2019].

[11] C. JW, S. PS, and G. EP, “Bacterial biofilms: a common cause of persistent infections,” *Science (80-.).*, vol. 284, no. May, p. 1318, 1999.

[12] W. Ziebuhr, S. Hennig, M. Eckart, H. Kränzler, C. Batzilla, and S. Kozitskaya, “Nosocomial infections by Staphylococcus epidermidis: how a commensal bacterium turns into a pathogen,” *Int. J. Antimicrob. Agents*, vol. 28, no. SUPPL. 1, pp. 14–20, 2006.

[13] W. H. Song, S. R. Hyun, and S. H. Hong, “Antibacterial properties of Ag (or Pt)-containing calcium phosphate coatings formed by micro-arc oxidation,” *J. Biomed. Mater. Res. - Part A*, vol. 88, no. 1, pp. 246–254, 2009.

[14] T. Theivasanthi and M. Alagar, “Studies of Copper Nanoparticles Effects on Micro-organisms,” 2011.

[15] A. Mandal and A. Cashin-Gerbutt, “What is Staphylococcus Aureus?,” *News Medical Life Sciences*, 2018. [Online]. Available: https://www.news-medical.net/health/What-is-Staphylococcus-Aureus.aspx. [Accessed: 03-Nov-2018].

[16] J. Seladi-Schulman and A. Pietrangelo, “E. Coli infection,” *Healthline.RED*, 2017. [Online]. Available: https://www.healthline.com/health/e-coli-infection. [Accessed: 15-Dec-2018].

[17] R. E. W. Hancock, “Resistance Mechanisms in *Pseudomonas aeruginosa* and Other Nonfermentative Gram-Negative Bacteria,” *Clin. Infect. Dis.*, vol. 27, no. s1, pp. S93–S99, 1998.

[18] M. Czajka, K. Sawicki, K. Sikorska, S. Popek, M. Kruszewski, and L. Kapka-Skrzypczak, “Toxicity of titanium dioxide nanoparticles in central nervous system,” *Toxicol. Vitr.*, vol. 29, no. 5, pp. 1042–1052, 2015.

[19] W. D. Callister Jr and D. G. Rethwisch, *Materials Science and Engineering*, 9th ed. John Wiley & Sons, 2011.

[20] K. Rokosz, T. Hryniewicz, and S. Raaen, “Development of plasma electrolytic oxidation for improved Ti6Al4V biomaterial surface properties,” *Int. J. Adv. Manuf. Technol.*, vol. 85, no. 9–12, pp. 2425–2437, 2016.

[21] T. K. Monsees *et al.*, “Effects of different titanium alloys and nanosize surface patterning on adhesion, differentiation, and orientation of osteoblast-like cells,” *Cells Tissues Organs*, vol. 180, no. 2, pp. 81–95, 2005.

[22] M. A. Elias, C.N., Lima, J.H.C., Valiev, R., and Meyers, “Biomedical applications of titanium and its alloys Biological Materials Science 46-49,” no. March, pp. 1–4, 2008.

[23] S. D. COOK, K. A. THOMAS, J. F. KAY, and M. JARCHO, “Hydroxyapatite-Coated Titanium for Orthopedic Implant Applications,” *Clin. Orthop. Relat. Res.*, vol. NA;, no. 232, p. 225???243, 1988.

[24] H. D. D. Michael, “Zirconia Dental Implants vs Titanium Implants,” *Sarasota Dentistry*, 2018. [Online]. Available: https://www.sarasotadentistry.com/dental-blog/zircona-dental-implants-vs-titanium-implants/. [Accessed: 02-Feb-2019].

[25] C. P. D. Morrison, “METAL IMPLANT LIABILITY INVIGORATES ADVANCES IN POLYMER ALTERNATIVES,” 2012. [Online]. Available: http://www.rjlg.com/2012/10/metal-implant-liability-invigorates-advances-in-polymer-alternatives/. [Accessed: 02-Feb-2019].

[26] B. Jackson, “FDA CLEARS ‘FIRST EVER’ 3D PRINTED SPINE IMPLANT TO TREAT MULTIPLE INJURIES,” 2018. [Online]. Available: https://3dprintingindustry.com/news/fda-clears-first-ever-3d-printed-spine-implant-treat-multiple-injuries-127509/. [Accessed: 02-Feb-2019].

[27] H. E. KH. Buchholz, “Über die Depotwirkund einiger Antibiotika bei Vermischung mit dem Kunstharz Palacos,” *Chirurg*, vol. 41, pp. 511–515, 1970.

[28] Y.-C. Ha, K.-H. Koo, S.-T. Jeong, J. Joon Yoo, Y.-M. Kim, and H. J. Kim, “Cementless Alumina-on-Alumina Total Hip Arthroplasty in Patients Younger Than 50 Years: A 5-year Minimum Follow-Up Study,” *J. Arthroplasty*, vol. 22, no. 2, pp. 184–188, 2007.

[29] S. Radin, J. T. Campbell, P. Ducheyne, and J. M. Cuckler, “Calcium phosphate ceramic coatings as carriers of vancomvcin,” *Biomaterials*, vol. 18, pp. 777–782, 1997.

[30] Y. Shinto, A. Uchida, F. Korkusuz, N. Araki, and K. Ono, “Calcium hydroxyapatite ceramic used as a delivery system for antibiotics,” *J. bone Jt. Surg.*, vol. 74–B, 1992.

[31] L. P. Barrere F, van Blitterswijk CA, de Groot K, “Influence of ionic strength and carbonate on the Ca-P coating formation from SBFx5 solution,” *Biomaterials*, vol. 23, pp. 1921–1930, 2002.

[32] M. Lucke *et al.*, “Gentamicin coating of metallic implants reduces implant-related osteomyelitis in rats,” *Bone*, vol. 32, no. 5, pp. 521–531, May 2003.

[33] O. P. Edupuganti *et al.*, “Covalent bonding of vancomycin to Ti6Al4V alloy pins provides long-term inhibition of Staphylococcus aureus colonization,” *Bioorganic Med. Chem. Lett.*, vol. 17, no. 10, pp. 2692–2696, 2007.

[34] B. Jose, V. Antoci Jr., A. R. Zeiger, E. Wickstorm, and N. J. Hickok, “Vancomycin Covalently Bonded to Titanium Beads Kills Staphylococcus aureus,” *Chem. Biol.*, vol. 12, pp. 1041–1048, 2005.

[35] P. Haesman, L. Haesman, F. Stacey, and G. McCracken, “Local delivery of chlorhexidine gluconate (PerioChip) in periodontal maintenance patients.,” *Clin Periodontol*, vol. 28, pp. 90–95, 2001.

[36] “Chlorhexidine,” *Pubchem, open chemistry database*. [Online]. Available: https://pubchem.ncbi.nlm.nih.gov/compound/chlorhexidine#section=Top. [Accessed: 05-Nov-2018].

[37] L. Harris, L. Mead, E. Muller-Oberlander, and R. Richards, “Bacteria and cell cytocompatibility studies on coated medical grade titanium surfaces.,” *Biomed Mater Res A*, vol. 78, pp. 50–58, 2008.

[38] M. Morra *et al.*, “Adsorption of cationic antibacterial on collagen-coated titanium implant devices.,” *Biomed Pharmacother*, vol. 58, pp. 418–422, 2004.

[39] W. Salem *et al.*, “Antibacterial activity of silver and zinc nanoparticles against Vibrio cholerae and enterotoxic Escherichia coli,” *Int. J. Med. Microbiol.*, vol. 305, no. 1, pp. 85–95, 2015.

[40] K. Reichelt and X. Jiang, “THE PREPARATION OF THIN FILMS BY PHYSICAL VAPOUR DEPOSITION METHODS,” vol. 191, pp. 91–126, 1990.

[41] A. Ewald, S. K. Glückermann, R. Thull, and U. Gbureck, “Antimicrobial titanium / silver PVD coatings on titanium,” vol. 10, pp. 1–10, 2006.

[42] J. C. B. Alcazar *et al.*, “Electrochemical cathodic polarization, a simplified method that can modified and increase the biological activity of titanium surfaces: A systematic review,” *PLoS One*, vol. 11, no. 7, pp. 1–17, 2016.

[43] X. Huang *et al.*, “One-step fabrication of cytocompatible micro/nano-textured surface with TiO2 mesoporous arrays on titanium by high current anodization,” *Electrochim. Acta*, vol. 199, pp. 116–125, 2016.

[44] Z. Q. Yao *et al.*, “Synthesis and properties of hydroxyapatite-containing porous titania coating on ultrafine-grained titanium by micro-arc oxidation,” *Acta Biomater.*, vol. 6, no. 7, pp. 2816–2825, 2010.

[45] “MC3T3-E1 Cell Line from mouse,” *Sigma-Aldrig, Merck*, 2018. [Online]. Available: https://www.sigmaaldrich.com/catalog/product/sigma/cb_99072810?lang=en&region=BE. [Accessed: 07-Nov-2018].

[46] P. Zhang, Z. Zhang, and W. Li, “Antibacterial TiO2coating incorporating silver nanoparticles by microarc oxidation and ion implantation,” *J. Nanomater.*, vol. 2013, 2013.

[47] I. Sondi and B. Salopek-Sondi, “Silver nanoparticles as antimicrobial agent: A case study on E. coli as a model for Gram-negative bacteria,” *J. Colloid Interface Sci.*, vol. 275, no. 1, pp. 177–182, 2004.

[48] R. Pati *et al.*, “Topical application of zinc oxide nanoparticles reduces bacterial skin

infection in mice and exhibits antibacterial activity by inducing oxidative stress response and cell membrane disintegration in macrophages," *Nanomedicine Nanotechnology, Biol. Med.*, vol. 10, no. 6, pp. 1195–1208, 2014.

[49] B. S. Necula, I. Apachitei, F. D. Tichelaar, L. E. Fratila-Apachitei, and J. Duszczyk, "An electron microscopical study on the growth of TiO2-Ag antibacterial coatings on Ti6Al7Nb biomedical alloy," *Acta Biomater.*, vol. 7, no. 6, pp. 2751–2757, 2011.

[50] S. M. Hussain, K. L. Hess, J. M. Gearhart, K. T. Geiss, and J. J. Schlager, "In vitro toxicity of nanoparticles in BRL 3A rat liver cells," *Toxicol. Vitr.*, vol. 19, no. 7, pp. 975–983, 2005.

[51] X. Yao, X. Zhang, H. Wu, L. Tian, Y. Ma, and B. Tang, "Microstructure and antibacterial properties of Cu-doped TiO2 coating on titanium by micro-arc oxidation.," *Appl. Surf. Sci.*, vol. 292, pp. 944–947, 2004.

[52] J. Konieczny and Z. Rdzawski, "Antibacterial properties of copper and its alloys Antibacterial properties of copper and its alloys," *Arch. Mater. Sci. Eng.*, vol. 56, no. 2, pp. 53–60, 2012.

[53] R. Burgers and R. van Boekel, "Zink heeft twee gezichten," no. 1, pp. 14–16, 2014.

[54] M. M. Mohamed, S. A. Fouad, H. A. Elshoky, G. M. Mohammed, and T. A. Salaheldin, "Antibacterial effect of gold nanoparticles against Corynebacterium pseudotuberculosis," *Int. J. Vet. Sci. Med.*, vol. 5, no. 1, pp. 23–29, 2017.

[55] Y. Zhou, Y. Kong, S. Kundu, J. D. Grillo, and H. Liang, "Antibacterial activities of gold and silver nanoparticles against Escherichia coli and bacillus Calmette-Guérin," *J. Nanobiotechnology*, vol. 10, pp. 1–9, 2012.

[56] K. Rokosz and T. Hryniewicz, "Plasma Electrolytic Oxidation as a modern method to form porous coatings enriched in phosphorus and copper on biomaterials," vol. 35, pp. 44–61, 2016.

[57] "Physical Electroncis - XPS / ESCA," 2019. [Online]. Available: https://www.phi.com/surface-analysis-techniques/xps-esca.html. [Accessed: 17-Mar-

2019].

[58] A. G. Skirtach, W. H. De Vos, and W. Van Criekinge, *Quantitative cell biology*. 2018.

[59] “International Organization for Standardization,” 2017. [Online]. Available: https://www.iso.org/standard/36406.html. [Accessed: 17-May-2019].

[60] L. Zhang, J. Guo, X. Huang, Y. Zhang, and Y. Han, “The dual function of Cu-doped TiO2 coatings on titanium for application in percutaneous implants,” *J. Mater. Chem. B*, vol. 4, no. 21, pp. 3788–3800, 2016.

[61] “Wikipedia,” 2019. [Online]. Available: https://en.wikipedia.org/wiki/Titanium. [Accessed: 09-May-2019].

[62] D. P. Smethurst and H. C. Williams, “The hardest known oxide,” *Br. Commun.*, vol. 410, p. 2, 2001.

FACULTY OF ENGINEERING AND ARCHITECTURE

Development of antibacterial TiO_2 coatings on titanium implants by plasma electrolytic oxidation

Renee Coryn
Student number: 01408564

Supervisors: Prof. dr. ir. Nathalie De Geyter, Prof. dr. ir. Kim Verbeken
Counsellor: Monica Thukkaram

Master's dissertation submitted in order to obtain the academic degree of
Master of Science in Biomedical Engineering

Academic year 2018-2019

GHENT UNIVERSITY